tube containing a homogenous, incompressible, and nonviscous liquid. When this tube is disturbed at one place, the disturbance will be propagated as waves along the tube at a finite speed. The problem is to determine this speed.

Let us impose some further simplifications.* Let the wave amplitude be small and the wave length be long compared with the tube radius, so that the slope of the deformed wall remains $\ll 1$ at all times. Under these conditions we can introduce an important hypothesis that the flow is essentially one dimensional, with a longitudinal velocity component $u(x, t)$, which is a function of the axial coordinate x and time t. In comparison with u, other velocity components are negligibly small. Then the basic equations can be obtained from the general equations listed in Section 2.6. They are the equation of continuity (or conservation of mass),

$$\frac{\partial A}{\partial t} + \frac{\partial}{\partial x}(uA) = 0, \tag{1}$$

and the equation of motion,

$$\frac{\partial u}{\partial t} + u\frac{\partial u}{\partial x} + \frac{1}{\rho}\frac{\partial p_i}{\partial x} = 0. \tag{2}$$

Here $A(x, t)$ is the cross-sectional area of the tube and $p_i(x, t)$ is the pressure in the tube. The relationship between p_i and A may be quite complex. For simplicity we introduce another hypothesis, that A depends on the transmural pressure, $p_i - p_e$, alone,

$$p_i - p_e = P(A), \tag{3}$$

where p_e is the pressure acting on the outside of the tube. Equation (3) is a gross simplification. In the theory of elastic shells we know that the tube deformation is related to the applied load by a set of partial differential equations and that the external load includes the inertial force of the tube wall (see Eqs. (4) and (5) of Sec. 3.15). Hence Eq. (3) implies that the mass of the tube is ignored and that the partial differential equations are replaced by an algebraic equation. By assuming Eq. (3) the dynamics of the tube is replaced by statics. The viscoelasticity of tube wall is ignored.

In the theoretical development, the derivative of the function $P(A)$ is very important, particularly in the following combination,

$$c = \sqrt{\frac{A}{\rho}\frac{dP}{dA}}. \tag{4}$$

We shall see later that c is the velocity of propagation of progressive waves.

These equations are not difficult to solve since Georg Riemann (1826–1866) has shown the way. But before solving these equations we shall

* In subsequent sections we shall relax these assumptions and evaluate their effects.

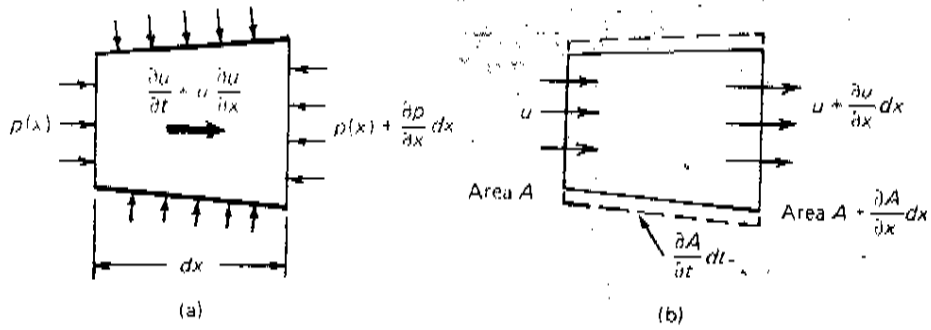

FIGURE 3.8:1. Free-body diagram of an arterial element, showing pressure, velocity, and wall displacement.

derive them once more from elementary considerations to make sure that we know them well.

Consider first the balance of forces acting in the axial direction on a fluid element of length dx and cross-sectional area A. A free-body diagram is shown in Figure 3.8:1(a). Since the fluid is nonviscous there is no shear stress acting on it. The force acting on the left end due to the pressure is pA toward the right; that acting on the right end is $[p + (\partial p/\partial x)dx][A + (\partial A/\partial x)dx]$ toward the left. The pressure acting on the lateral sides contributes an axial force $p(\partial A/\partial x)dx$ toward the right. Therefore, on neglecting the second-order term, the net pressure force is $A(\partial p/\partial x)dx$ acting toward the left. The mass is $\rho A\,dx$, with ρ being the density of the blood. According to Newton's law the net force will cause an acceleration $\partial u/\partial t + u\partial u/\partial x$. On equating the force with mass times acceleration, we obtain Eq. (2).

Next, consider the conservation of mass in a segment of the tube of length dx, as illustrated in Figure 3.8:1(b). In a unit time the mass influx at the left end is equal to ρuA; the efflux at the right is $\rho\{uA + [\partial(uA)/\partial x]dx\}$. In the mean time the volume of the element is increased by $(\partial A/\partial t)dx$. The law of conservation of mass then leads to Eq. (1).

Next, consider the elasticity of the tube. If the tube behaves like a pulmonary artery or vein, then the situation is simple. The pulmonary arterial diameter $2a_i$ is linearly proportional to the blood pressure in the vessel p_i (see Sec. 6.7):

$$2a_i = 2a_{i0} + \alpha p_i, \tag{5}$$

where a_{i0} and α are constants that depend on the pleural pressure p_{PL} and the airway pressure p_A, but are independent of blood pressure p_i. α is the compliance constant of the vessel, and a_{i0} is the radius when $p_i = 0$. Differentiation of Eq. (5) then yields the relationship

$$da_i = \frac{\alpha}{2}dp_i. \tag{6}$$

Equations (1), (2), and (6) govern the wave propagation phenomenon. Let us first solve a linearized version of these equations. Consider small disturbances in an initially stationary liquid-filled circular cylindrical tube. In this case u is small and the second term in Eq. (2) can be neglected. Hence

$$\frac{\partial u}{\partial t}+\frac{1}{\rho}\frac{\partial p_i}{\partial x}=0. \tag{7}$$

The area A is equal to πa_i^2. Substituting πa_i^2 for A in Eq. (1), remembering the hypothesis that the wave amplitude is much smaller than the wave length, so that $\partial a_i/\partial x \ll 1$, then, on neglecting small quantities of the second order, we can reduce Eq. (1) to the form

$$\frac{\partial u}{\partial x}+\frac{2}{a_i}\frac{\partial a_i}{\partial t}=0. \tag{8}$$

Combining Eqs. (8) and (6), we obtain

$$\frac{\partial u}{\partial x}+\frac{\alpha}{a_i}\frac{\partial p_i}{\partial t}=0. \tag{9}$$

Differentiating Eq. (7) with respect to x and Eq. (9) with respect to t, subtracting the resulting equations, and neglecting the second order term $(\alpha/a_i^2)(\partial a_i/\partial t)(\partial p_i/\partial t)$, we obtain

$$\frac{\partial^2 p_i}{\partial x^2}-\frac{1}{c^2}\frac{\partial^2 p_i}{\partial t^2}=0, \tag{10}$$

where

$$c^2=\frac{a_i}{\rho\alpha}. \tag{11}$$

Equation (10) is the famous *wave equation*. The quantity c is the *wave speed*,

$$c=\sqrt{\frac{a_i}{\rho\alpha}}. \tag{12}$$

The derivation of Eq. (12) is simple because the pressure-diameter relationship Eq. (5) is simple. The derivation of wave speed for blood vessels that obey more complex pressure-diameter relationships is given below.

Wave Speed in Thin-Walled Elastic Tube

If the tube is thin walled and the material obeys Hooke's law, then for a small change in radius da_i the circumference is changed by $2\pi da_i$ and the circumferential strain is $2\pi da_i/2\pi a_i = da_i/a_i$. If E is the Young's modulus of the wall material the circumferential stress is changed by the amount Eda_i/a_i. If the wall thickness is h, the tension in the wall is changed by $Ehda_i/a_i$. This increment of tension is balanced by the change of pressure

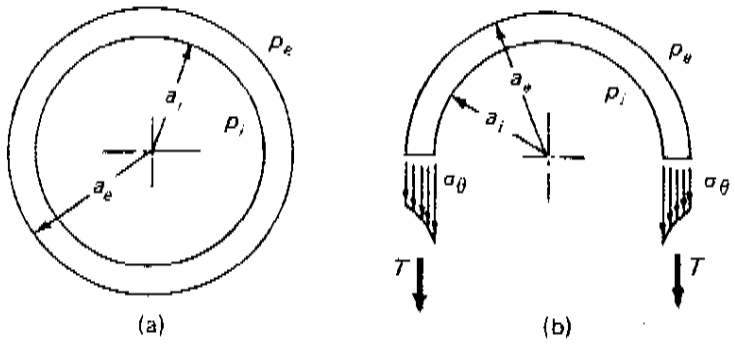

FIGURE 3.8.2. The balances of forces in an arterial wall.

dp_i. According to the condition of equilibrium of the forces acting on a free body shown in Figure 3.8.2(b), we have

$$\frac{Ehda_i}{a_i} = a_i dp_i. \tag{13}$$

This equation is of the same form as Eq. (6) with

$$\frac{\alpha}{2} = \frac{a_i^2}{Eh}. \tag{14}$$

The wave speed in such a tube is, therefore,

$$c = \sqrt{\frac{Eh}{2\rho a_i}}. \tag{15}$$

This formula was first derived by Thomas Young in 1808, and is known as the Moens–Korteweg formula, because it was popularized and modified by Korteweg (1878). Moens (1878).

Note that if the thin-wall assumption is not made the accuracy of the result can be improved by computing the strain on the midwall of the tuber, $a_i/(a_i + h/2)$. Then the wave speed is

$$c = \sqrt{\frac{Eh}{2\rho\left(a_i + h/2\right)}}. \tag{16}$$

Wave Speed in Arteries with Nonlinear Elasticity

More realistic constitutive equations of arteries are given in Eqs. (40)–(51) of Section 2.6; and are discussed in greater detail in (Fung, 1993b, Chap. 8). Let the internal and external radii of the vessel be a_i and a_e, respectively, and the corresponding pressures be p_i and p_e (see Fig. 3.8.2(a)). Let the radii be a_{i0} and a_{e0} when the pressures p_i and p_e are zero. The condition of equi-

librium of the forces acting on a free body shown in Figure 3.8:2(b) yields the average circumferential stress,

$$\langle \sigma_\theta \rangle = (p_i a_i - p_e a_e)/(a_e - a_i). \tag{17}$$

Let us define the stretch ratio λ_θ and strain $E_{\theta\theta}$ on the midwall by the formulas

$$\lambda_\theta = \frac{a_i + a_e}{a_{i0} + a_{e0}}, \quad E_{\theta\theta} = \frac{1}{2}(\lambda_\theta^2 - 1). \tag{18}$$

Then, if $\rho_0 W^{(2)}$ denotes the strain energy function in the arterial wall expressed as a function of the strains $E_{\theta\theta}$ and E_{zz} (the longitudinal strain), we have (Fung, 1993b, Sec. 7.11 and 8.6)

$$\langle \sigma_\theta \rangle = \lambda_\theta^2 \frac{\partial(\rho_0 W^{(2)})}{\partial E_{\theta\theta}}. \tag{19}$$

Combining Eqs. (17) and (19) we have

$$p_i a_i - p_e a_e = (a_i - a_e)\lambda_\theta^2 \frac{\partial(\rho_0 W^{(2)})}{\partial E_{\theta\theta}}. \tag{20}$$

The function $\rho_0 W^{(2)}$ is given by Fung, Fronek, Patitucci (1979) and in Fung (1993b, Sec. 8.6, Eq. (3)):

$$\rho_0 W^{(2)} = \frac{1}{2} C' \exp\left[a_1 E_{\theta\theta}^2 + a_2 E_{zz}^2 + 2a_4 E_{\theta\theta} E_{zz}\right], \tag{21}$$

where C', a_1, a_2, a_4 are constants. The radii a_i and a_e are related by the condition of incompressibility of the wall,

$$\pi(a_e^2 - a_i^2) = \pi(a_{e0}^2 - a_{i0}^2). \tag{22}$$

On computing $\partial a_e/\partial a_i$ from Eq. (22) and using it in an equation obtained by differentiating Eq. (20), we obtain

$$\begin{aligned} a_i\, dp_i + p_i\, da_i - p_e \frac{a_i}{a_e} da_i = {} & \lambda_\theta^2 \frac{\partial(\rho_0 W^{(2)})}{\partial E_{\theta\theta}} \left(1 - \frac{a_i}{a_e}\right) da_i \\ & + (a_i - a_e) \frac{\partial}{\partial \lambda_\theta} \left[\lambda_\theta^2 \frac{\partial(\rho_0 W^{(2)})}{E_{\theta\theta}}\right] \frac{d\lambda_\theta}{da_i} da_i. \end{aligned} \tag{23}$$

This can be put in the form of Eq. (6) if we identify

$$\begin{aligned} \frac{2}{\alpha} = {} & -\frac{p_i}{a_i} + \frac{p_e}{a_e} + \left(\frac{1}{a_i} - \frac{1}{a_e}\right) \lambda_\theta^2 \frac{\partial(\rho_0 W^{(2)})}{\partial E_{\theta\theta}} \\ & + \left(\frac{a_i}{a_e} - \frac{a_e}{a_i}\right) \frac{\partial}{\partial \lambda_\theta} \left[\lambda_\theta^2 \frac{\partial \rho_0 W^{(2)}}{\partial E_{\theta\theta}}\right]. \end{aligned} \tag{24}$$

The compliance α varies obviously with p_i, p_e, and a_i. If only infinitesimal disturbances da_i, dp_i, dp_e are considered, then the quantity on the right-hand side of Eq. (24) can be evaluated at the steady state and used as a constant in Eq. (11). In that case the linearized wave equation (10) applies.

Solution of the Wave Equation

To understand the nature of the phenomenon described by differential Eq. (10), let us take the following mathematical approach. Let $f(z)$ be an arbitrary function of z, which is differentiable at least twice and whose second derivative is continuous for a certain prescribed region of z. Let z be a function of two variables x and t,

$$z = x - ct, \tag{25}$$

where x represents the coordinate of a point on a straight line and t represents time. Now, by the rules of differentiation, we have

$$\frac{\partial f}{\partial x} = \frac{df}{dz}\frac{\partial z}{\partial x} = \frac{df}{dz}, \quad \frac{\partial f}{\partial t} = \frac{df}{dz}\frac{\partial z}{\partial t} = -c\frac{df}{dz},$$
$$\frac{\partial^2 f}{\partial x^2} = \frac{d^2 f}{dz^2}, \quad \frac{\partial^2 f}{\partial t^2} = c^2\frac{d^2 f}{dz^2}. \tag{26}$$

The last line shows that the function $f(x - ct)$ satisfies the differential equation

$$\frac{\partial^2 f}{\partial x^2} - \frac{1}{c^2}\frac{\partial^2 f}{\partial t^2} = 0,$$

which is exactly Eq. (10). Thus Eq. (10) is solved by $p = f(x - ct)$.

Now suppose that a disturbance occurs at time $t = 0$ over a segment of the vessel as illustrated in Figure 3.8:3. The amplitude of the disturbance is represented by $f(x)$ at $t = 0$. At a time t_1 later, the same disturbance will appear translated to the right. The value of the disturbance $f(x - ct)$ will remain constant as long as $x - ct$ has the same value; hence an increase in t requires an increase in $x = ct$. Thus the function $f(x - ct)$ represents a wave propagating to the right (in the direction of increasing x) with a speed c. In exactly the same manner, we can shown that $f(x + ct)$ satisfies the wave equation and represents a wave moving in the negative x direction with a speed c.

Flow Velocity and Wall Displacement Waves

Equation (10) shows that the pressure in the elastic vessel is governed by a wave equation. Because the axial velocity u is linearly related to p through Eq. (7), and small change of the radius, a, is linearly related to changes in p through Eq. (6), (13), or (23), we see that u and a are governed by the

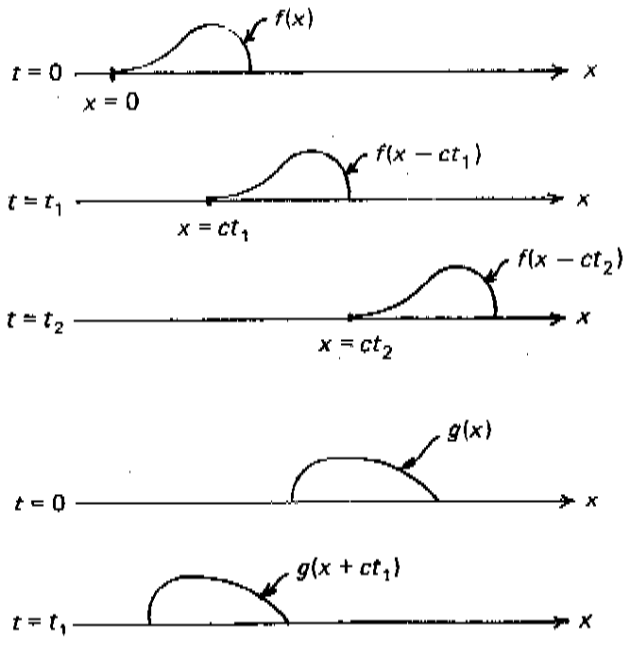

FIGURE 3.8:3. Wave propagation to the right and left.

same wave equation with the same wave speed. In other words, the p in Eq. (10) can be replaced by u and a. (Verify this by direct differentiation.) Thus disturbances in velocity and radius of the vessel are propagated by waves of speed c, in association with the pressure wave.

We use pulse waves in arteries of the wrist, ankle, or temple to determine the heart rate. If we press very gently on the artery, we feel the pulsation of the radius of the artery. If we press harder, so that an area of the artery under the finger is flattened, we should feel the pressure wave in the artery (Fung, 1993b, p. 20, Prob 1.5). With a Doppler ultrasound flow meter, you can detect the velocity waves.

Our derivation of the wave equation is subjected to many simplifying assumptions. All the factors ignored in this derivation have some effect on real wave propagation in the arteries. We discuss them in due course.

Relationship Between the Pressure and Velocity Waves

We have argued that the pressure and velocity satisfy the same wave equation. We can show that the wave equation is satisfied by

$$\begin{aligned} p &= p_o f(x-ct) + p_o' g(x+ct), \\ u &= u_o f(x-ct) + u_o' g(x+ct), \end{aligned} \tag{27}$$

and that by Eq. (7) or (9) the *amplitudes p_o and u_o are related by the simple relationship*

$$p_o = \rho c u_o \tag{28}$$

for a wave that is moving in the positive x direction, and

$$p_o' = -\rho c u_o' \tag{29}$$

for a wave that moves in the negative x direction.

The proof is very simple. On substituting Eq. (27) into Eq. (7), carrying out the differentiation and cancelling the common factor df/dz, we obtain Eq. (28) or (29).

This important relationship shows *that the amplitude of the pressure wave is proportional to the product of wave speed, velocity disturbance, and the fluid density, and nothing else.* This conclusion holds for progressive waves in long tubes without reflection. This, incidentally, is a general result for one-dimensional longitudinal waves, which may occur, for example, in a car crash, or in a plane compressional wave in the earth during earthquake.

Problems on Series Representation of Waves (Fig. 3.8:4)

3.13 Consider a half-sine pulse,

$$f(x) = \sin\frac{\pi x}{L} \quad \text{for} \quad 0 \le x \le L,$$
$$f(x) = 0 \quad \text{for} \quad x < 0, \quad x > L,$$

propagating to the right at speed c. Sketch the wave after 1 s.

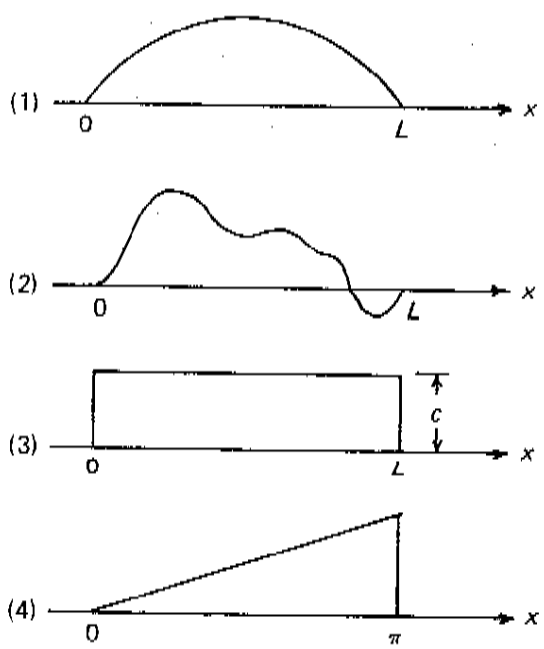

FIGURE 3.8:4. Several wave forms.

3.14 If at time $t = 0$ a wave is observed to have a spatial distribution

$$f(x) = \sum_{n=1}^{\infty} a_n \sin\frac{n\pi x}{L} \quad \text{for} \quad x \text{ in } (0, L) \tag{30}$$

and $f(x) = 0$ outside this interval, show that at time t the solution of wave Eq. (14) is

$$f(x \pm ct) = \sum_{n=1}^{\infty} a_n \sin\frac{n\pi}{L}(x \pm ct) \tag{31}$$

for $x \pm ct$ in $(0, L)$, and $f(x \pm ct) = 0$ elsewhere. The $\pm$ sign is chosen according to whether the direction of propagation is to the left (+) or right (−).

If a wave described by Eq. (31) propagating to the right is observed at a fixed station $x = 0$, then the time sequence is

$$f(-ct) = -\sum_{n=1}^{\infty} a_n \sin\frac{n\pi c}{L}t. \tag{32}$$

Each term in Eq. (32) is a *harmonic* of the wave. The nth is called the *nth harmonic*. The factor $n\pi c/L$ is the *frequency* (or more precisely, *circular frequency*) of the nth harmonic of the pulse wave.

3.15 Show that a square wave of amplitude c in the region $0 < x < L$ can be represented by

$$f(x) = c = \frac{4c}{\pi}\left(\sin\frac{\pi x}{L} + \frac{1}{3}\sin\frac{3\pi x}{L} + \frac{1}{5}\sin\frac{5\pi x}{L} + \cdots\right), \tag{33}$$

whereas one in the region $-L/2 < x < L/2$ can be represented by

$$f(x) = c = \frac{4c}{\pi}\left(\cos\frac{\pi x}{L} - \frac{1}{3}\cos\frac{3\pi x}{L} + \frac{1}{5}\cos\frac{5\pi x}{L} - \cdots\right). \tag{34}$$

Both of these formulas hold for the open intervals indicated. At the ends $x = 0$ and L, the Gibbs phenomenon occurs: The value represented by the series oscillates about c.

3.16 Show that a triangular wave $f(x) = x$ in $-\pi < x < \pi$ can be represented as

$$f(x) = x = 2\left(\sin x - \frac{\sin 2x}{2} + \frac{\sin 3x}{3} - \frac{\sin 4x}{4} + \cdots\right) \tag{35}$$

whereas in $0 \le x \le \pi$, inclusive, we have

$$f(x) = x = \frac{\pi}{2} - \frac{4}{\pi}\left(\cos x + \frac{\cos 3x}{3^2} + \frac{\cos 5x}{5^2} + \frac{\cos 7x}{7^2} + \cdots\right). \tag{36}$$

Note the difference in the rate of convergence of the series that represents the same function.

Mathematical Choices of Series to Represent a Function

The choice of the series expansions, as illustrated in Problems 3.15 and 3.16, seems arbitrary, but there are beautiful theorems, such as the following. If one chose to represent a function in the range $-1 \le x \le 1$ by a series of *ultraspherical polynomials* (Szegö, 1939), which includes powers of x, Legendre polynomials, Chebyshev polynomials, and others, then, as Lanczos (1952) has shown, *if the series is truncated at n terms, the estimated error of an expansion into Chebyshev polynomials is smaller than that of any other expansion into ultraspherical polynomials. While the expansion into powers of x (Taylor series) gives the slowest convergence, the expansion into Chebyshev polynomials gives the fastest convergence.*

In case the reader is not familiar with the Chebyshev polynomial, remember that it is nothing but the simple trigonometric function $\cos k\theta$, but expressed in the variable

$$x = \cos\theta.$$

Thus, the Chebyshev polynomial $T_k(x)$ is

$$T_k(x) = \cos(k \operatorname{arc}\cos x). \tag{37}$$

What is meant by this theorem is that if a function $f(x)$ of bounded variation is expanded into a series

$$f(x) = \tfrac{1}{2}c_0 + c_1T_1(x) + c_2T_2(x) + \cdots + c_nT_n(x) + \eta_n(x), \tag{38}$$

then the maximum value of the remainder η_n is smaller than that of any other expansions in which $T_k(x)$ is replaced by other ultraspherical polynomials. If the expansion (38) is rearranged into an ordinary power series of the form

$$f(x) = b_0 + b_1x + b_2x^2 + \cdots + b_nx^n + \eta_n'(x), \tag{39}$$

then the coefficients b_i decrease slower than the coefficients c_i as i increases and the maximum of the remainder $\eta_n'(x)$ is greater than that of $\eta_n(x)$. In fact, the convergence of the power series in Eq. (39) is the slowest among all expansions in ultraspherical polynomials.

This theorem shows that an orthogonal expansion of $f(x)$ into the polynomials $T_k(x)$ yields an expansion that for the same number of terms represents $f(x)$ with greater accuracy than the expansion into any other sets of orthogonal functions (this includes the Legendre polynomials, which give a better average error but a worse maximum error in the given range).

An Example of Harmonic Analysis of Pulse Waves

In Figure 3.8:5, experimental data on pressure and flow in the ascending aorta of a dog are shown by dotted curves. These curves are analyzed into a Fourier series with a constant term and 10 harmonics (with frequencies

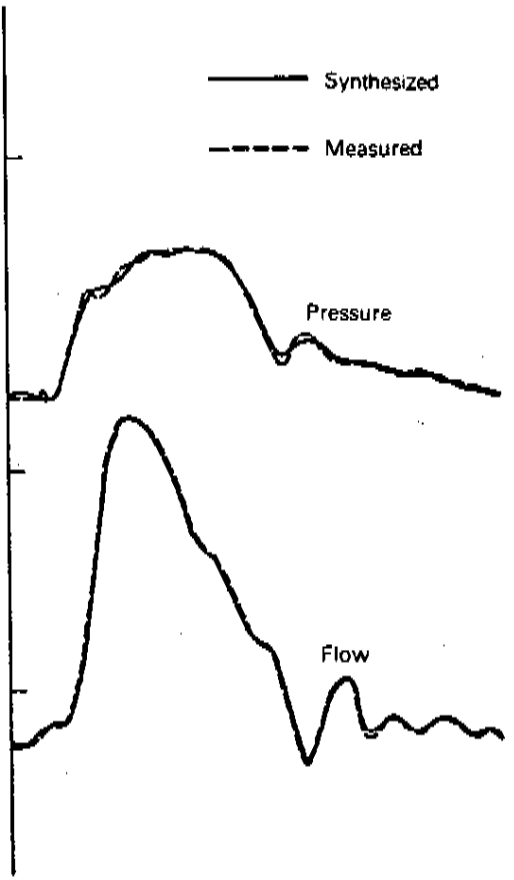

FIGURE 3.8:5. An example of Fourier series representation of pressure and flow waves in the ascending aorta. The experimental wave form is analyzed into a Fourier series with 10 harmonics. The series is then summed and plotted, showing good agreement with experimental data. From McDonald (1974), by permission.

up to about 20 Hz). The solid curves represent the Fourier series. It is shown that the accuracy of the 10-harmonic approximation is acceptable. Further away from the heart, the wave forms are smoother and can be adequately described by fewer harmonics.

3.9 Progressive Waves Superposed on a Steady Flow

The results derived so far apply to a straight, cylindrical, elastic tube filled with a nonviscous liquid that is not flowing. Now, we shall continue to assume the fluid to be nonviscous, but let it have a steady flow to the right. Since the fluid is nonviscous, the no-slip condition on the solid wall does not apply. The velocity profile can be uniform. Then we can show that all equations of Section 3.8 are applicable provided that we adopt a coordinate system that moves with the undisturbed flow, and interpret u as the perturbation velocity superposed on the steady flow and c as the

speed of perturbation wave relative to the undisturbed flow. The proof is as follows:

Let U be the velocity of the undisturbed flow and u the small perturbation superposed on it. Treating u as an infinitesimal quantity of the first order, we see that the equation of motion, Eq. (3.8:2), can be linearized into

$$\frac{\partial u}{\partial t} + U\frac{\partial u}{\partial x} = -\frac{1}{\rho}\frac{\partial p_i}{\partial x}. \tag{1}$$

This can be reduced to Eq. (3.8:7) by introducing a transformation of variables from x, t to x', t':

$$x' = x - Ut, \quad t' = t. \tag{2}$$

From Eq. (2) we have

$$\begin{aligned} \frac{\partial}{\partial t} &= \frac{\partial}{\partial t'}\frac{\partial t'}{\partial t} + \frac{\partial}{\partial x'}\frac{\partial x'}{\partial t} = \frac{\partial}{\partial t'} - U\frac{\partial}{\partial x'}, \\ \frac{\partial}{\partial x} &= \frac{\partial}{\partial t'}\frac{\partial t'}{\partial x} + \frac{\partial}{\partial x'}\frac{\partial x'}{\partial x} = \frac{\partial}{\partial x'}. \end{aligned} \tag{3}$$

Hence, a substitution into Eq. (1) reduces it to

$$\frac{\partial u}{\partial t'} = -\frac{1}{\rho}\frac{\partial p}{\partial x'}, \tag{4}$$

which is exactly Eq. (3.8:7) in the new coordinates.

The equation of continuity, Eq. (3.8:1), now becomes

$$\frac{\partial a_i}{\partial t} + U\frac{\partial a_i}{\partial x} + \frac{a_i}{2}\frac{\partial u}{\partial x} = 0 \tag{5}$$

when πa_i^2 is substituted for A, with a_i being the inner radius of the tube, and $U + u$ is substituted for u and the equation is linearized for small perturbations. Under the transformation Eq. (2), and using Eq. (5), Eq. (6) becomes

$$\frac{\partial a_i}{\partial t'} + \frac{a_i}{2}\frac{\partial u}{\partial x'} = 0, \tag{6}$$

which is exactly Eq. (3.8:8).

The pressure–radius relationship—Eq. (3.8:5), (3.8:6), (3.8:13), or (3.8:23)—is independent of reference coordinates; thus Eq. (3.8:9) is unchanged when t is replaced by t'. Thus all the basic equations are unchanged. Equations (4) and (6) govern the fluid and Eq. (3.8:9) governs the tube and fluid interaction, that is, the boundary conditions. By eliminating u, the same wave equation (3.8:10) is obtained, except that the independent variables are replaced by x' and t'. But x' and t' are the distance and time measured in the moving coordinates that translate with the undisturbed flow. Thus what we set out to prove is done.

Can Boundary Layers Save the Ideal Fluid Theory?

The wave theory of Section 3.8 is an ideal fluid theory. The superposition of a uniform velocity is valid for an ideal fluid only, not for blood which is viscous. A viscous fluid must obey the no-slip condition. The question is: Could the boundary layer theory discussed in Section 3.5 save the ideal fluid solution for the bulk of blood in the vessel, leaving the boundary layer to adjust to the no-slip condition on vessel wall? Heuristically, the answer is "yes," if the Reynolds and Womersley numbers are large and the vessel is not too long, so that the boundary layers are very thin compared with the tube radius. The short length requirement is related to the boundary layer thickness growth discussed in Section 3.18.

For blood flow in large arteries, in which the Reynolds and Womersley numbers are $\gg 1$, pulse wave analysis of ideal fluid flow provides a good approximation. Hence, we continue to use the ideal fluid hypothesis in the study of wave propagation, reflection, and refraction in large arteries in Sections 3.10 to 3.13. For waves in small arteries and arterioles, in which either the Womersley number, or the Reynolds number, or both approach 1 or <1, we must take viscosity into account, as is done in Section 3.15.

Experimental Validation

Experimental evidence of the theoretical result is shown in Figure 3.9:1. Anliker et al. (1968) installed two electromagnetic wave generators at two stations along a dog aorta and recorded the pressure fluctuations at two points between the two wave generators. A short train of high-frequency waves generated by the upstream wave generator propagates downstream with a theoretical velocity

$$c^D = c + U, \tag{7}$$

which can be determined experimentally by the arrival times of the wave train at the two recording stations. On the other hand, if the wave train is generated by the downstream generator and propagated upstream, the theoretical wave speed is

$$c^U = c - U, \tag{8}$$

which again can be determined experimentally. From Eqs. (7) and (8) we have

$$U = \tfrac{1}{2}\left(c^D - c^U\right). \tag{9}$$

In Figure 3.9:1, c^D, c^U, and U are shown during a cardiac cycle. The flow velocity U can also be measured by a flow gauge, and as Anliker stated, a good agreement is obtained.

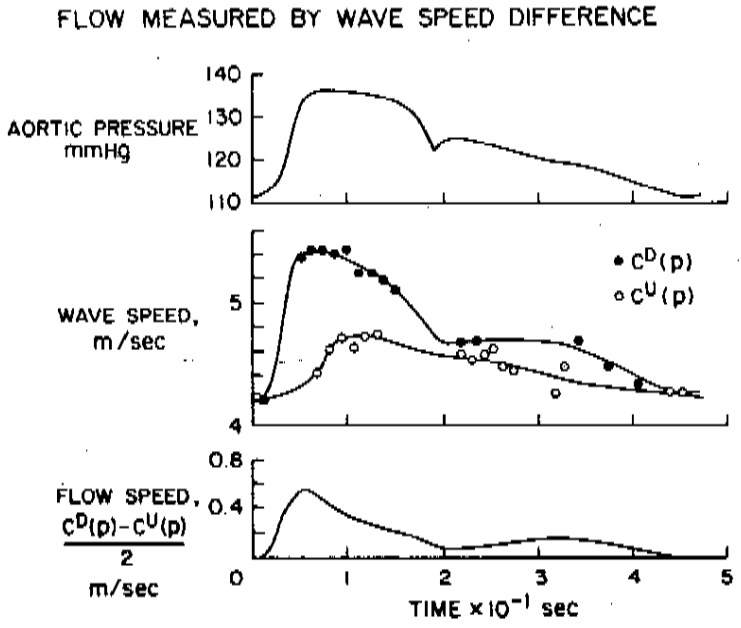

FIGURE 3.9:1. Wave speeds measured upstream and downstream in the aorta of a dog. *Top:* Natural pulse wave. *Middle:* Upstream wave speed (open symbols) and downstream wave speed (closed symbols) measured at different instants of the cardiac cycle. The upstream and downstream data correspond to two heartbeats a few seconds apart, but with matching pressure patterns. *Bottom:* Mean flow velocity U. From Anliker, M. (1972), by permission.

3.10 Nonlinear Wave Propagation

A more general solution of Eqs. (1), (2), and (3) of Section 3.8 is given by Riemann's method of characteristics. This method is explained most clearly in Lighthill (1978), and Yih (1977). Adding $\pm c/A$ times Eq. (1) of Section 3.8 to Eq. (2) of Section 3.8, one can show that on the characteristic curves defined by

$$dx/dt = u \pm c, \tag{1}$$

the quantities (Riemann invariants)

$$R_{\pm} = \frac{1}{2}\left[u \pm \int_{A_0}^{A} \frac{c}{A}\, dA\right] \tag{2}$$

are constants, where A_0 is the undisturbed area and c is the velocity

$$c^2 = \frac{A}{\rho}\frac{dp}{dA}. \tag{3}$$

Thus nonlinear waves are propagated in the $\pm x$ directions with speeds $u \pm c$. The linearlized theory presented in Section 3.8 results if the condition $c \gg u$ is imposed.

The general solution, Eq. (2), can be used to investigate the effect of some of the simplifying assumptions used in the preceding section. It has been used by Pedley (1980, pp. 79–87) to investigate the formation of shock waves in blood vessels.

The method of characteristics is one of the most important devices to investigate nonlinear wave propagation. See Lighthill (1978), and Skalak (1966, 1972) for in-depth reviews of this subject. Lambert (1958) averaged the equations of motion and continuity over the arterial cross section to obtain uniaxial equations. Van der Werff (1973) introduced a special method to handle periodic conditions. Atabek (1980) combined the characteristics method with Ling and Atabek's (1972) "local flow" analysis to predict velocity profiles of the flow and waves in a segment from known pressure and pressure gradient at the proximal end of the segment. Atabek's detailed comparison between calculated results and those from animal experiments shows the importance of the effects of nonlinearity from various sources (see Sec. 3.16 in this book); he concludes that these effects are not yet fully understood.

Problem

3.17 We know that the blood vessel wall does not obey Hooke's law. Use the information on the pseudo-elasticity and viscoelasticity of the arteries presented in *Biomechanics: Mechanical Properties of Living Tissues* (Fung, 1993b, chapter 8) to derive an expression for the wave speed in arteries.

Devise a theory of your own to handle the viscoelasticity of the blood vessel wall in the problem of pulse wave propagation. Discuss the effect of viscoelasticity in detail.

3.11 Reflection and Transmission of Waves at Junctions of Large Arteries

Thus far we have discussed propagation of uniaxial disturbances in an infinitely long, straight, cylindrical, elastic tube filled with an incompressible nonviscous liquid. Our results are simple and interesting, but they are true only if all the idealizing qualifiers hold. Real arteries do not obey these qualifiers: They are short, tapered, branching, and filled with a non-Newtonian viscous fluid. They are sometimes curved. Their walls are nonlinearly viscoelastic. It turns out that in the large arteries the effect of nonlinear viscoelasticity on wave propagation is not so severe; neglecting the blood viscosity in the tube outside the boundary layer next to the wall is often acceptable for the wave propagation problem because the frequency para-

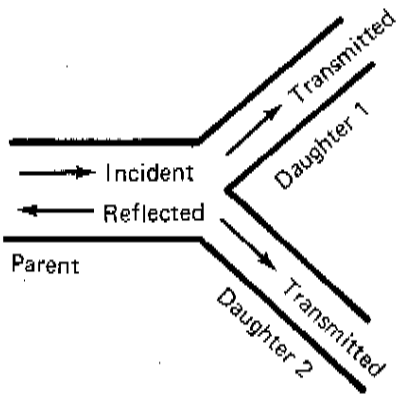

FIGURE 3.11:1. A bifurcating artery.

meter (Sec. 3.7) α and the Reynolds number N_R are sufficiently large that the boundary layer is very thin (we will discuss these factors later), but the "infinitely long" assumption must be removed.

A tube of finite length must have two ends. When waves of pressure and velocity reach an end, they must conform to the end conditions. As a result the waves will be modified. To clarify the situation, consider first a single junction, as shown in Figure 3.11:1, where a tube branches into two daughters. A wave traveling down the parent artery will be partially reflected at the junction and partially transmitted down the daughters. Now, at the junction, the conditions are as follows:

a. The pressure is a single-valued function.
b. The flow must be continuous.

To express this mathematically, let p_I denote the oscillatory pressure associated with the incident wave, p_R that associated with the reflected wave, and p_{T_1} and p_{T_2} those associated with the transmitted waves in the two daughter tubes; then according to (a) we must have

$$p_I + p_R = p_{T_1} = p_{T_2}. \tag{1}$$

Similarly, let $\dot{Q}$ denote the volume-flow rate, and let the subscripts I, R, T_1, T_2 refer to the various waves as before; then, according to (b) we must have

$$\dot{Q}_I - \dot{Q}_R = \dot{Q}_{T_1} + \dot{Q}_{T_2}. \tag{2}$$

The left-hand side of Eq. (2) represents the flow out of the parent tube, and the right-hand side represents the flow into the daughters. But $\dot{Q}$ is just the product of the cross-sectional area A and the mean velocity u. We have already learned the relationship between u and p in Section 3.8. Hence, using Eq. (3.8:28) and Eq. (3.8:29) we obtain the flow–pressure relationship,

$$\dot{Q} = Au = \pm \frac{A}{\rho c} p. \tag{3}$$

Here ρ is the density of the blood and c is the wave speed. The + sign applies if the wave goes in the direction of positive x-axis; the – sign applies if the wave goes the other way. The quantity $\rho c/A$ is an important characteristic of the artery and is called the *characteristic impedance* of the tube, and is denoted by the symbol Z,

$$Z = \frac{\rho c}{A}. \tag{4}$$

Z is the ratio of oscillatory pressure to oscillatory flow when the wave goes in the direction of positive x-axis,

$$Z = \frac{p}{\dot{Q}}, \quad Z\dot{Q} = p, \tag{5}$$

analogous to the resistance in an electric circuit,

$$R = \frac{V}{I}, \quad RI = V, \tag{6}$$

connecting the voltage V and current I. Z has the physical dimensions $[ML^{-4}T^{-1}]$ and can be measured in the units $\mathrm{kg\,m^{-4}\,sec^{-1}}$. With the Z notation, Eq. (2) can be written as

$$\frac{p_I - p_R}{Z_0} = \frac{p_{T_1}}{Z_1} + \frac{p_{T_2}}{Z_2}. \tag{7}$$

Solving Eqs. (1) and (7) for the p's, we obtain

$$\frac{p_R}{p_I} = \frac{Z_0^{-1} - \left(Z_1^{-1} + Z_2^{-1}\right)}{Z_0^{-1} + \left(Z_1^{-1} + Z_2^{-1}\right)} = \mathscr{R} \tag{8}$$

and

$$\frac{p_{T_1}}{p_I} = \frac{p_{T_2}}{p_I} = \frac{2Z_0^{-1}}{Z_0^{-1} + \left(Z_1^{-1} + Z_2^{-1}\right)} = \mathscr{T}. \tag{9}$$

The right-hand sides of Eqs. (8) and (9) shall be denoted by $\mathscr{R}$ and $\mathscr{T}$, respectively. Hence the amplitude of the reflected pressure wave at the junction is $\mathscr{R}$ times that of the incident wave, the amplitude of the transmitted pressure waves at the junction is $\mathscr{T}$ times the incident wave. The amplitude of the reflected velocity wave is, however, equal to $-\mathscr{R}$ times that of the incident velocity wave, because the wave now moves in the negative x-axis direction, and according to Eqs. (3.8:28) and (3.8:29), there is a sign change in the relation between u and p depending on whether the waves move in the + or – x-axis direction.

The meaning of $\mathscr{R}$ and $\mathscr{T}$ can be clarified further by considering the transmission of energy by pressure waves. Imagine a cross section of the tube. The normal stress acting on this section is the pressure p. The force is

p times the area, A. The fluid pushed by this pressure moves at a velocity u. The rate at which work is done is therefore the product pAu. But $Au = \dot{Q}$ and $\dot{Q} = p/Z$. Therefore the rate of work done is

$$\dot{W} = p\dot{Q} = p^2/Z. \tag{10a}$$

This is the rate of transmission of mechanical energy through the cross section. Now, at the junction of a bifurcating vessel, the rate of energy transmission of the incident wave is p_I^2/Z_0, whereas that of the reflected wave is

$$\frac{p_R^2}{Z_0} = \frac{\left(\mathcal{R}p_I\right)^2}{Z_0} = \mathcal{R}^2\,\frac{p_I^2}{Z_0}. \tag{10b}$$

Hence the ratio of the rate of energy transmission of the reflected wave to that of the incident wave is $\mathcal{R}^2$. For this reason $\mathcal{R}^2$ is called the *energy reflection coefficient*. Similarly, the rate of energy transfer in the two transmitted waves, compared with that in the incident wave, is

$$\frac{Z_1^{-1} + Z_2^{-1}}{Z_0^{-1}}\mathcal{T}^2, \tag{10c}$$

which is called the *energy transmission coefficient*.

We can express the waves more explicitly as follows. Let the incident wave be

$$p_I = p_0 f\left(t - x/c_0\right). \tag{11}$$

Let the junction be located at $x = 0$, so that x is negative in the parent tube and positive in the daughter tubes; then at the junction, $x = 0$, the pressure of the incident wave is

$$p_I = p_0 f\left(t\right).$$

The reflectional and transmitted waves are, therefore,

$$\begin{aligned} p_R &= \mathcal{R}p_0 f\left(t + x/c_0\right), \\ p_{T_1} &= \mathcal{T}\,p_0 f\left(t - x/c_1\right), \\ p_{T_2} &= \mathcal{T}\,p_0 f\left(t - x/c_2\right). \end{aligned} \tag{12}$$

Here c_0, c_1, c_2 are the wave speeds in the respective tubes. Note that $p_{T_1} = p_{T_2}$ at the junction, $x = 0$ [see Eq. (1)], but c_1 may be different from c_2. The resultant disturbance in the parent tube is

$$p = p_I + p_R = p_0 f\left(t - x/c_0\right) + \mathcal{R}p_0 f\left(t + x/c_0\right). \tag{13}$$

The corresponding flow disturbance in the parent tube is, according to Eq. (3) and taking the direction of propagation into account,

$$\dot{Q} = \frac{Ap_0}{\rho c_0} f\left(t - x/c_0\right) - \mathcal{R}\frac{Ap_0}{\rho c_0} f\left(t + x/c_0\right). \tag{14}$$

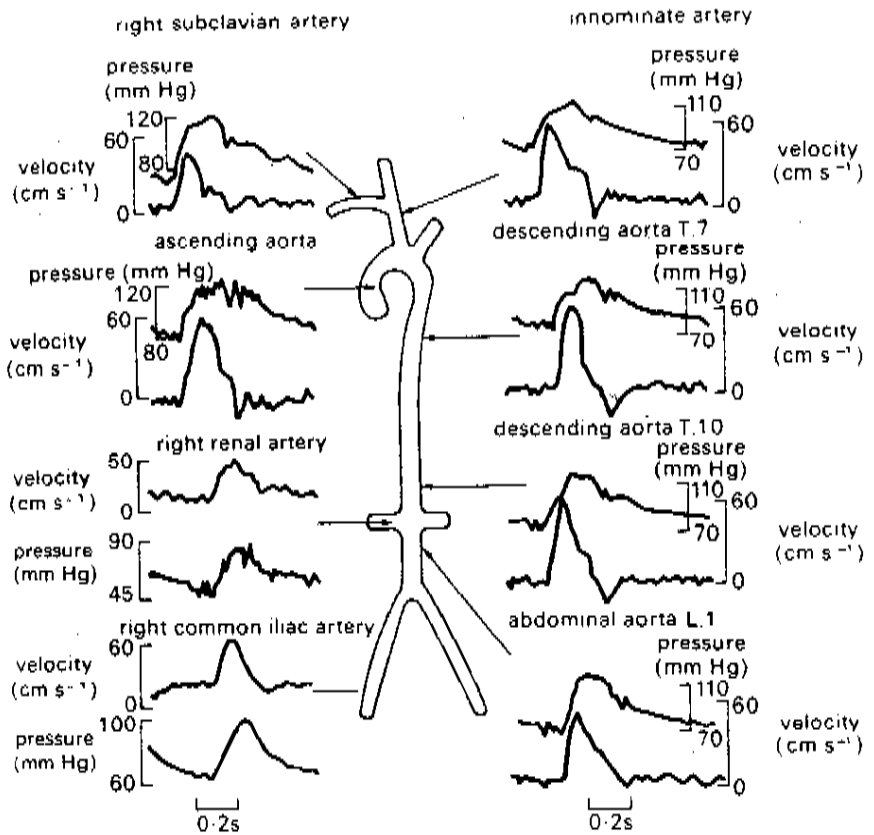

FIGURE 3.11:2. Pressure and flow waves in human arterial tree. From Mills et al. (1970) Pressure-flow relationships and vascular impedance in man. *Cardiovascular Res.* **4**: 405–417, by permission.

A comparison of Eqs. (13) and (14) shows that with reflection, the pressure and flow wave forms are no longer equal.

Inequality of pressure and flow wave forms is a common feature of pulse waves in arteries (Fig. 3.11:2), indicating the effect of reflection at branches.

Problems

3.18 Consider the case in which a parent tube gives rise to three daughter tubes at a junction. Show that $\mathscr{R}$ and $\mathscr{T}$ are given by expressions similar to Eqs. (8) and (9), except that $Z_1^{-1} + Z_2^{-1}$ should be replaced by $Z_1^{-1} + Z_2^{-1} + Z_3^{-1}$ (Fig. P3.18).

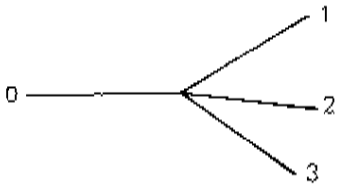

FIGURE P3.18. Trifurcation.

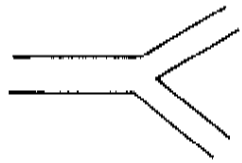

FIGURE P3.19. Matched impedance.

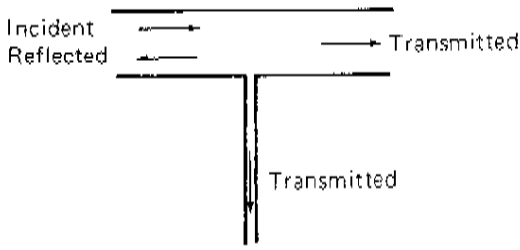

FIGURE P3.20. A small daughter branch.

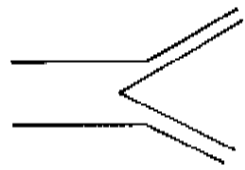

FIGURE P3.21. Total reflection.

3.19 Under what condition is the reflected wave zero? State the condition $\mathscr{R} = 0$ in terms of the physical parameters of the tubes.

Note: When $\mathscr{R} = 0$ the junction is said to be one at which the *impedances* are matched (Fig. P3.19).

A parent tube gives out a small daughter branch (Fig. P3.20). What are reflection and transmission characteristics ($\mathscr{R}$ and $\mathscr{T}$) at the junction?

Under what condition would a wave be totally reflected ($\mathscr{R} = 1$) (Fig. P3.21)?

If the impedance of a parent tube is perfectly matched to the daughter tubes at a junction so that $\mathscr{R} = 0$, show that $\mathscr{T} = 1$ and the transmission coefficient given in Eq. (10c) is 1. Show that $1 + \mathscr{R} = \mathscr{T}$.

3.20 Consider a bifurcating artery (see Fig. 3.11:1). The functions $\mathscr{T}$ [Eq. (9)] and $\mathscr{R}$ are called, respectively, the *transmission* and the *reflection coefficient* (without the word *energy*). In the special case in which the two daughter branches are of equal size and the wave speed c is the same in the parent and daughter branches, $\mathscr{R}$ and $\mathscr{T}$ are functions of the "area ratio," $(A_1 + A_2)/A_0$, that is, the ratio of the combined area of the branches to the area of the parent tube. Derive expressions of $\mathscr{R}$ and $\mathscr{T}$ in terms of the area ratio and sketch curves to show the variation of $\mathscr{R}$ and $\mathscr{T}$ with the area ratio.

Note: Cf. Atabek (1980), p. 302, in which the viscosity of the blood and viscoelasticity of the vessel wall are considered (see Sec. 3.15 *infra*), while the motion is limited to be simple harmonic (see p. 161).

Our results, Eqs. (4) to (10c), are derived for inviscid fluid in an elastic tube. Whereas the wave speed c is a real number in Eq. (4), it is a complex number in Atabek (see Sec. 3.15). Figure 7.16 of Atabek (1980) shows that there is a minor dependence of the magnitude of $\mathcal{R}$ and $\mathcal{T}$ on the Womersley number (α), and a sudden change of the phase angle of $\mathcal{R}$ (from 0 to 180°) when the area ratio exceeds about 1.2 to 1.4.

3.21 Design an instrument to measure pulse waves noninvasively at some conveniently located arteries, such as the radial artery at the wrist. What can you measure? Pressure? Force? Velocity? What significant use can be made of such measurements? (See Sec. 3.20.)

3.22 There are several machines in clinical use that apply pressure or vacuum on arteries of the arms or legs in a suitable periodic manner to serve as heart assist devices. One machine works on veins to reduce the threat of thrombosis. Invent one yourself, and explain why is it good.

Harmonic Waves

Oscillations that are sinusoidal in time and space are called *harmonic waves*. For example, a pressure wave,

$$p = p_0 \cos\left\{\omega\left(t - \frac{x}{c_0}\right)\right\} = p_0 \cos\left(\omega t - \frac{2\pi x}{\lambda}\right)$$

$$= p_0 \cos\left\{\frac{2\pi}{\lambda}\left(x - c_0 t\right)\right\}, \tag{15}$$

is a harmonic progressive wave. Here ω is the *circular frequency* (unit, rad/sec), $\omega/2\pi$ is the *frequency* (unit, Hz), and λ is the *wave length*, (unit, m). They are related by

$$\lambda = \frac{c_0}{(\omega/2\pi)}, \quad \frac{\omega}{2\pi} = \frac{c_0}{\lambda}. \tag{16}$$

Thus the wave length is the wave speed divided by frequency, or the distance traveled per cycle. The wave speed is the product of frequency and wave length.

For harmonic waves, a convenient mathematical device is the *complex representation*. This is based on the relation

$$e^{iz} = \cos z + i \sin z, \tag{17}$$

where $i = \sqrt{-1}$, e is the exponential function, and z is a real variable. Thus $\cos z$ is the real part of e^{iz} and $\sin z$ is the imaginary part of e^{iz}. We can write Eq. (15) as

$$p = \mathcal{R}\ell\left\{p_0 e^{i\omega(t-x/c_0)}\right\}. \tag{18}$$

The symbol $\mathcal{R}\ell$ means the real part of the complex quantity. A great advantage of the complex representation is that in Eq. (18) p_0 does not have to be limited to a real number. If p_0 is a complex number,

$$p_0 = a + ib = Pe^{i\phi},$$
$$P = \sqrt{a^2 + b^2}, \quad \phi = \tan^{-1}\frac{b}{a};$$

then Eq. (18) means

$$\begin{aligned} p &= a\cos\left\{\omega\left(t - x/c_0\right)\right\} - b\sin\left\{\omega\left(t - x/c_0\right)\right\} \\ &= P\cos\left\{\omega\left(t - x/c_0\right) + \phi\right\}. \end{aligned} \tag{19}$$

Hence P is the *amplitude* and ϕ is the *phase angle* of the wave. Similar expressions can be written for the flow rate and for waves traveling in the opposite direction. It is conventional to omit the symbol $\mathcal{R}\ell$, so that whenever a complex number is used to represent a physical quantity, it is assumed that its real part is being used.

We shall use this method to discuss multiple reflections later.

Problem

3.23 Consider energy transmission. We have shown in Eq. (10) that the rate of energy transmission in a progressive wave is

$$W = Ap \cdot u = p \cdot \dot{Q} = p^2/Z.$$

If p is a harmonic wave, show that this is

$$W = \mathcal{R}\ell p \cdot \mathcal{R}\ell\dot{Q} = \left(\mathcal{R}\ell p\right)^2/Z$$

and is not equal to $\mathcal{R}\ell(p^2)/Z$. This important example shows that one has to be careful in using the complex representation.

Show that if p is given by Eq. (15) the average value of W over a period is

$$W = \tfrac{1}{2}p_0^2/Z.$$

Multiple Reflections

Waves in more complex systems of tubes can be analyzed by repeated application of the results presented earlier. For example, in the double junction illustrated in Figure 3.11:3, a wave reflected once at junction B is reflected a second time at junction A, and so on. The amplitudes of the reflected and transmitted waves on each occasion are determined by the characteristics of the junction.

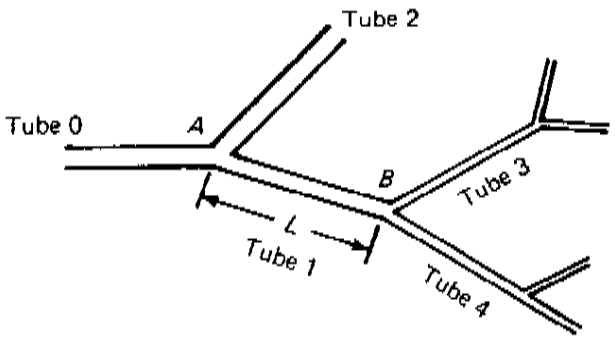

FIGURE 3.11:3. Multiple reflection sites of an artery with two branching junctions.

To see what is going on, let us consider a continuous harmonic excitation and write out in detail the perturbations in the segment AB. Let the origin of the x-axis be taken at A. Let the first wave transmitted through A be

$$p_1 e^{i\omega(t-x/c_0)}. \tag{20}$$

At B, where x = L, the pressure due to this wave is

$$p_1 e^{i\omega(t-L/c_0)}.$$

Here the wave is reflected. Let the reflection parameter be denoted by $\mathcal{R}_{10}$. Then the reflected wave is

$$\mathcal{R}_{10} p_1 e^{i\omega\left[t-L/c_0+(x-L)/c_0\right]}. \tag{21}$$

When this wave reaches A, the pressure is

$$\mathcal{R}_{10} p_1 e^{i\omega(t-2L/c_0)}.$$

This wave is reflected at A. To calculate the reflection parameter we must treat the segment AB as the parent tube and tubes 0 and 2 as daughters. Let the reflection parameters be denoted by $\mathcal{R}_{01}$. Then the reflected wave is

$$\mathcal{R}_{01}\mathcal{R}_{10} p_1 e^{i\omega(t-2L/c_0-x/c_0)}.$$

The process continues. The pressure perturbation in the tube AB is the sum of all these waves.

But the story cannot end here. At the ends A and B, the waves do not just bounce back and forth; they are also transmitted into the vessels beyond them, to segments 0, 2, 3, 4, etc. These transmitted waves will be reflected at the junctions further away and will come back to segment AB. The total picture will not be known until the entire system is accounted for. In practice, if the impedance is reasonably well matched, the series converges rapidly.

Standing Waves

The reflection and trapping of waves are related to the phenomenon of resonance. Consider a particular condition in which the tube AB is closed at both ends so that $\mathscr{R}_{10}$ and $\mathscr{R}_{13}$ are both equal to 1. In this case the sum of the first two waves, Eqs. (20) and (21), becomes, with Eq. (16),

$$e^{i(\omega t - 2\pi x/\lambda)} + e^{i\left[\omega t - 2\pi L/\lambda + 2\pi(x-L)/\lambda\right]}.$$

The sum of every two succeeding terms is similar, differing only in phase angle. In the special case in which the tube length is equal to the half-wave length,

$$L = \frac{\lambda}{2}, \tag{22}$$

the sum above becomes (because $e^{-i2\pi}$ is equal to 1)

$$e^{i\omega t}\left\{e^{-i\pi x/L} + e^{i\pi x/L}\right\} = 2e^{i\omega t}\cos\frac{\pi x}{L}. \tag{23}$$

Thus, in this case the oscillation is a standing wave, and the motion is a *resonant vibration*. This occurs at a frequency of

$$\frac{\omega}{2\pi} = \frac{c_0}{\lambda} = \frac{c_0}{2L} = \frac{1}{2L}\sqrt{\frac{Eh}{2\rho a}}, \tag{24}$$

which is said to be the *fundamental frequency* of natural vibration; Eq. (23) is said to be the *fundamental mode*. If a system is excited at a resonance frequency, the amplitude of vibration can only be limited by damping. Higher modes are obtained if $L = \lambda/(2n)$, where n is an integer, in which case the mode shape is $\cos 2\pi nx/L$ and the frequency is n times the fundamental.

Real use of this concept is limited. The vibration mode and natural frequency depend on the end conditions. Any change of the end conditions changes the modes. The mode (23) corresponds to a tube with closed ends. Open the ends and the mode is changed.

3.12 Effect of Frequency on the Pressure–Flow Relationship at any Point in an Arterial Tree

The complex branching pattern of the arteries tells us at once that multiple reflections of pulse waves must be a major feature of blood flow. The differences between the pressure and flow profiles shown in Figure 3.11:2 quoted in the preceding section support this statement because, if it were not for the reflections, the pressure and flow waves would have similar profiles. But if reflection is important, then the flow and pressure relationship

at any given site in the artery must depend on how the multiple reflections at the bifurcation points are seen at this site, how far away the bifurcation point is, and how long it takes for each wave to travel from a bifurcation point to that site. At any given time, the pressure and flow at a given site are the sums of the newly arrived waves and the retarded waves of reflection from earlier fluctuations. This means that the pressure–flow relationship is frequency dependent.

To express the frequency-dependent characteristics of an arterial tree, it is customary to consider each harmonic of the pulse wave separately and to write, at a given site and a given frequency, the ratio of pressure to flow:

$$\frac{p}{\dot{Q}} = Me^{i\theta} = Z_{\text{eff}}. \tag{1}$$

p and $\dot{Q}$ are represented by complex numbers multiplied by $e^{i\omega t}$. Their ratio is, of course, a complex number, and is called the *input impedance* or *effective impedance*. Its modulus, M, is the ratio of the amplitudes of pressure and flow, whereas its argument, θ, is the phase lag of flow-rate oscillation behind the pressure oscillation.

The input impedance of the human arterial tree can be obtained by analyzing the measured pressure and velocity waves at a given site (e.g., one of those illustrated in Fig. 3.11:2) by Fourier series (e.g., Fig. 3.8:4), and computing the ratio of the corresponding complex-valued harmonics. An example of experimental input impedance measured in the ascending aorta is shown in Figure 3.12:1, which was taken from the same set of measurements as the wave forms shown in Figure 3.11:2. There is a minimum of M at a frequency of 3 Hz, and calculation shows that this implies the presence of a major reflection site roughly at the level of the aortic bifurcation. Measurements at different sites in the aorta lead to the same conclusion.

The input (or effective) impedance is not the same as the characteristic impedance of the tube in which the measurements are made. Don't use the word *impedance* without telling the reader what impedance you mean. The ratio of pressure to flow at any point is called the *effective impedance*. The effective impedance at a point A (see, e.g., Fig. 3.11:3) is called the *input impedance* of the system distal to A.

This terminology comes from electric circuit theory. If a circuit is connected to a voltage source and we want to know if the system can be operated successfully, we often need to know only the input impedance that the circuit offers to the source. Similarly, if we want to couple the arterial system to the heart, we need to know the input impedance of the arterial system at the aortic valve. If we want to know the function of the kidney, we want to know the input impedance of the kidney at the point where the renal artery branches from the abdominal aorta.

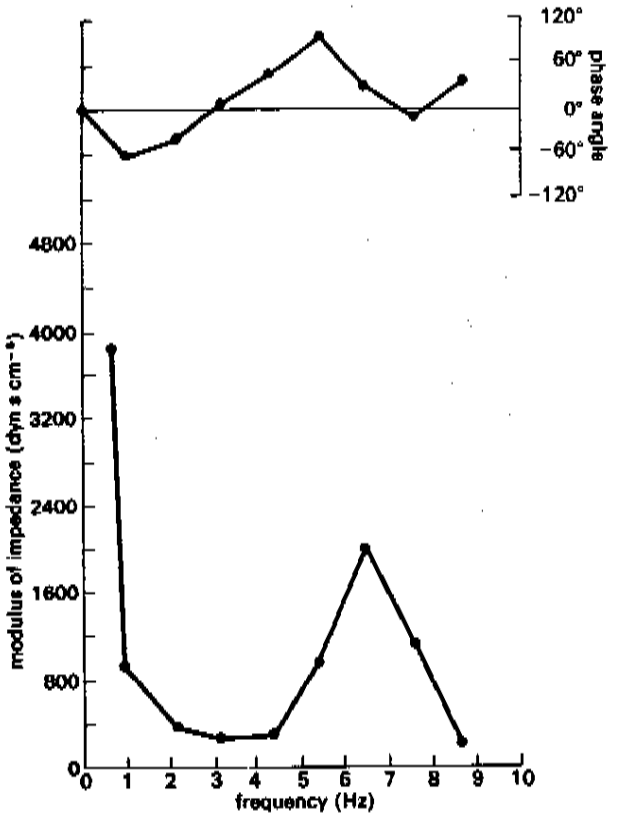

FIGURE 3.12:1. Input impedance of the human ascending aorta. The phase angle and modulus are plotted against the wave frequency. The single minimum of the modulus suggests that there is a single effective reflection site at the level of aortic bifurcation. From Mills et al. (1970) Pressure–flow relationships and vascular impedance in man. *Cardiovasc. Res.* **4**: 405–417, by permission.

Examples

1. *Input Impedance of a Branching Artery* (see Fig. 3.11:3). Consider an artery AB (segment 1) that branches into segments 3 and 4. Let a pressure wave $p_I e^{i\omega t}$ be imposed at the terminal A. A pressure wave $p_I e^{i\omega(t-x/c_1)}$ propagates to the right. When it reaches B at time $t = L/c_1$, it is reflected as a pressure wave,

$$p_R e^{i\omega\left[t-L/c_1-(L-x)/c_1\right]}, \tag{2}$$

propagating toward A, and is transmitted into segments 3 and 4 as progressive waves

$$p_{T_3} e^{i\omega\left(t-L/c_1-x_3/c_3\right)}, \quad p_{T_4} e^{i\omega\left(t-L/c_1-x_4/c_4\right)}, \tag{3}$$

respectively, where x_3, x_4 are distances measured from point B. Since the pressure at B is single valued, we have, on substituting $x = L$, $x_3 = x_4 = 0$ (at B) and cancelling the factors $e^{i\omega(t-L/c_1)}$ throughout,

$$p_I + p_R = p_{T_3} = p_{T_4}. \tag{4}$$

The flows associated with the incident and reflected waves in segment 1 are obtained by dividing the pressure waves with the characteristic impedance Z_1 of that segment. The flows into branches 3 and 4 are obtained by dividing the pressures at point B by the effective impedances $Z_{3\text{eff}}$ and $Z_{4\text{eff}}$, respectively. Hence, on equating the inflow with outflow at B and again cancelling the factor exp $[i\omega(t - L/c_1)]$,

$$\frac{1}{Z_1}p_I - \frac{1}{Z_1}p_R = \frac{p_{T_3}}{Z_{3\text{eff}}} + \frac{p_{T_4}}{Z_{4\text{eff}}}. \tag{5}$$

These equations are the same as those of Section 3.11, except that Z_3 and Z_4 are replaced by effective impedances. By solving these equations for p_R, p_{T_3}, and p_{T_4}, as before, we obtain

$$\frac{p_R}{p_I} = \mathscr{R}_{\text{eff}}, \quad \frac{p_{T_3}}{p_I} = \frac{p_{T_4}}{p_I} = \mathscr{T}_{\text{eff}}, \tag{6}$$

where

$$\mathscr{R}_{\text{eff}} = \frac{Z_1^{-1} - \left(Z_{3\text{eff}}^{-1} + Z_{4\text{eff}}^{-1}\right)}{Z_1^{-1} + \left(Z_{3\text{eff}}^{-1} + Z_{4\text{eff}}^{-1}\right)}, \quad \mathscr{T}_{\text{eff}} = 1 + \mathscr{R}_{\text{eff}}. \tag{7}$$

Note that this result is the same as that of Section 3.11 except for a change in notation and interpretation. In Section 3.11 we speak of progressive waves going through the bifurcation point B, anticipating the waves to be reflected at other points of bufurcation but discussing the situation at B before any of the reflected waves arrive at B. In the present section we consider periodic oscillations and allow the waves to be reflected and transmitted as the system permits and demands, and find that a progressive wave is reflected at a junction with a complex amplitude ratio $\mathscr{R}_{\text{eff}}$ when the characteristic impedances used in Section 3.11 are replaced by the effective impedances of the downstream branches.

Now, back at point A, where $x = 0$, let us assume that the reflected wave passes through without further reflection. Then the pressure and flow are

$$p_A = p_I e^{i\omega t} + p_R e^{i(\omega t - 2L\omega/c_1)} = p_I e^{i\omega t}\left(1 + \mathscr{R}_{\text{eff}}\, e^{-2i\omega L/c_1}\right), \tag{8}$$

$$Q_A = \frac{p_I}{Z_1} e^{i\omega t} - \frac{p_R}{Z_1} e^{i(\omega t - 2L\omega/c_1)} = p_I e^{i\omega t}\,\frac{1}{Z_1}\left(1 - \mathscr{R}_{\text{eff}}\, e^{-2i\omega L/c_1}\right). \tag{9}$$

Using Eq. (1), we obtain, finally, the ratio of p_A to Q_A, which is the input impedance at A:

$$\frac{p_A}{Q_A} = Z_{1\text{eff}} = Z_1 \frac{1+\mathcal{R}_{\text{eff}}\, e^{-2i\omega L/c_1}}{1-\mathcal{R}_{\text{eff}}\, e^{-2i\omega L/c_1}}. \tag{10}$$

We can recast the final result in a different form. On substituting Eq. (7) for $\mathcal{R}_{\text{eff}}$ into Eq. (10), multiplying both the numerator and denominator by $(Z_1^{-1} + Z_{3\text{eff}}^{-1} + Z_{4\text{eff}}^{-1})e^{i\omega L/c_1}$, and noting that for any α,

$$\frac{e^{i\alpha} + e^{-i\alpha}}{2} = \cos\alpha, \quad \frac{e^{i\alpha} - e^{-i\alpha}}{2} = i\sin\alpha, \tag{11}$$

we obtain the important result

$$Z_{1\text{eff}}^{-1} = Z_1^{-1} \frac{\left(Z_{3\text{eff}}^{-1} + Z_{4\text{eff}}^{-1}\right) + iZ_1^{-1}\tan\left(\omega L/c_1\right)}{Z_1^{-1} + i\left(Z_{3\text{eff}}^{-1} + Z_{4\text{eff}}^{-1}\right)\tan\left(\omega L/c_1\right)}. \tag{12}$$

By repeated use of this equation, we can obtain the effective impedance at any point, that is, the relationship between the oscillatory pressure and flow rate at that point, from their values at the distal ends.

The factor $\omega L/c_1$ is equal to $2\pi L/\lambda$, where λ is the wavelength $2\pi c_1/\omega$. If $\omega L/c_1 = n\pi$ (n an integer), then $\tan(\omega L/c_1) = 0$ and

$$Z_{1\text{eff}}^{-1} = Z_{3\text{eff}}^{-1} + Z_{4\text{eff}}^{-1}. \tag{13}$$

Thus, if the arterial length L is much smaller than the wavelength, then $n \to 0$ and Eq. (13) shows that the artery may be considered as part of the junction and there is no change of the pressure–flow relationship in that segment.

On the other hand, if $\omega L/c_1$ is equal to an odd multiple of $\pi/2$, that is, if L is equal to an odd multiple of quarter-wavelengths, then $\tan(\omega L/c_1) = \infty$ and

$$Z_{1\text{eff}}^{-1} = \frac{Z_1^{-2}}{Z_{3\text{eff}}^{-1} + Z_{4\text{eff}}^{-1}}. \tag{14}$$

In this case, if Z_1^{-1} is smaller (or greater) than $Z_{3\text{eff}}^{-1} + Z_{4\text{eff}}^{-1}$, then $Z_{1\text{eff}}^{-1}$ is smaller (or greater) than Z_1^{-1}.

2. *Reverberative Reflections in an Artery.* Consider an artery with two sites of reflection, A and B (see Fig. 3.11:3). A pressure wave $p_o e^{i(\omega t - kx)}$ enters at A. At B it is reflected with a change of amplitude. The reflected wave, on arriving at A, is reflected again, and so on. Let the ratio of the complex amplitude of the reflected wave to that of the incident wave be denoted by $\mathcal{R}_1$ at A and $\mathcal{R}_2$ at B (the subscripts "eff" being omitted for simplicity). Then, at a station at a distance x from A and at time t, the pressure is

$$\begin{aligned} p(x,t) = {} & p_o e^{i\omega(t-x/c)} + \mathcal{R}_2 p_o e^{i\omega\left[(t-L/c)-(L-x)/c\right]} \\ & + \mathcal{R}_1\mathcal{R}_2 p_o e^{i\omega\left[(t-2L/c)-x/c\right]} \\ & + \mathcal{R}_1\mathcal{R}_2^2 p_o e^{i\omega\left[(t-3L/c)-(L-x)/c\right]} + \cdots. \end{aligned} \tag{15}$$

We now assemble terms that represent waves going to the right and, separately, those representing waves going to the left. We obtain

$$p(x,t) = p_o e^{i\omega(t-x/c)}\left[1 + \mathcal{R}_1\mathcal{R}_2 e^{-i2\omega L/c} + \cdots\right] + \mathcal{R}_2 p_o e^{i\omega(t-2L/c+x/c)}\left[1 + \mathcal{R}_1\mathcal{R}_2 e^{-i2\omega L/c} + \cdots\right]. \tag{16}$$

Using the summation formula

$$1 + \alpha + \alpha^2 + \alpha^3 + \cdots = \frac{1}{1-\alpha}, \tag{17}$$

for whatever α, we obtain an important formula

$$p(x,t) = \frac{p_o e^{i\omega(t-x/c)} + \mathcal{R}_2 p_o e^{i\omega(t-2L/c+x/c)}}{1 - \mathcal{R}_1\mathcal{R}_2 e^{i2\omega L/c}}. \tag{18}$$

This is a general result. Now, consider the special case of total reflection at the two ends, $\mathcal{R}_1 = \mathcal{R}_2 = 1$. Then

$$p(x,t) = p_o e^{i\omega t}\frac{e^{-i\omega x/c} + e^{-i2\omega L/c}e^{i\omega x/c}}{1 - e^{-i2\omega L/c}}. \tag{19}$$

If we multiply the numerator and denominator by $e^{i\omega L/c}$ and use Eqs. (11), we obtain

$$p(x,t) = p_o e^{i\omega t}\frac{\cos\omega(L-x)/c}{i\sin(\omega L/c)}, \tag{20}$$

which represents a "standing" wave. The wave is "standing" because it does not propagate.

The amplitude of the standing wave will tend to infinity if the denominator sin ($\omega L/c$) tends to zero; then the oscillation is said to "resonate." This occurs if

$$\frac{\omega L}{c} = n\pi \quad \text{or} \quad L = n\frac{\lambda}{2} \quad (n = 1,2,\cdots), \tag{21}$$

that is, if the length of the segment equals an integral multiple of half-wavelength.

Problems

3.24 When the frequency tends to zero, show that the phase angle θ tends to zero and the modulus M tends to a constant. With suitable assumptions with regard to an arterial tree at the peripheral end (microcirculation), derive an expression for M as the frequency tends to zero.

Note: That the dynamics modulus of input impedance can be much smaller than the static impedance (resistance at zero frequency) is of great importance and interest. Compare this with some of our daily

experiences. We can often shake a small tree if we do it at the right frequency, whereas the tree would not deflect very much if the same force is applied statically. In the circulatory system, this means that we can get blood to move with much smaller driving pressure when it is done dynamically.

3.25 Explain why can we extract information on input impedance from measurements such as those illustrated in Figure 3.11:2. One may use the Fourier analysis approach (see Sec. 3.8, Example 2). Express both the pressure and flow wave forms in Fourier series, and then compare them with the complex representation of waves discussed in Section 3.11.

3.26 In Section 3.8, Example 5, we extolled Chebyshev polynomials as the basis of generalized Fourier series. Can you develop a formal theory of input impedance in terms of Chebyshev polynomials? What difficulty is there?

3.13 Pressure and Velocity Waves in Large Arteries

The pressure and flow waves in arteries are generated by the heart. The conditions at the aortic valve and the capillary blood vessels are the end conditions of the arterial system. Major features along the length of the large arteries are explainable by the simple analysis presented in preceding sections, but the explanation of the major features of flow in regions close to the aortic valve must take the three-dimensional geometry of the left ventricle, the valve, and the aorta into consideration, together with three-dimensional fluid dynamics and the dynamics of the solid structures involved. Similarly, the analysis of flow in regions of vessel bifurcation, atherosclerosis, aneurysm, stenosis, or dilatation require extensive numerical calculation. Some of these problems are discussed in Sections 3.14 to 3.19. Here we present some features of flow in the aorta.

Figure 3.13:1 shows simultaneous recordings of the pressure in the left ventricle and in the ascending aorta immediately downstream from the aortic valve. When heart contracts, pressure rises rapidly in the ventricle at the beginning of systole and soon exceeds that in the aorta, so that the aortic valve opens, blood is ejected, and aortic pressure rises. During the early part of the ejection, ventricular pressure exceeds aortic pressure. About halfway through ejection, the two pressure traces cross, and the heart is faced with an adverse pressure gradient. The flow and pressure start to fall. Then a notch in the aortic pressure record (the *dicrotic notch*) marks the closure of the aortic valve. Thereafter the ventricular pressure falls very rapidly as the heart muscle relaxes: The aortic pressure falls more slowly, with the elastic vessel serving as a reservoir. The major feature of the pressure wave in the aorta is explained by the windkessel theory (see Sec. 2.1),

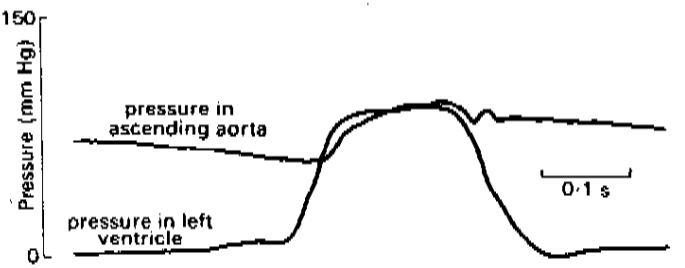

FIGURE 3.13:1. Pressure in the left ventricle and ascending aorta of the dog. From Noble, (1968) The contribution of blood momentum to left ventricular ejection in the dog. *Circ. Res.* **23**: 663–670. Reproduced by permission of the American Heart Association.

but the details can only be determined when all the waves are accounted for.

The change of pressure wave with distance from the aortic valve is shown in Figure 3.13:2. First we see a shift of the profile to the right, suggesting a wave propagation. We also see a steepening and increase in amplitude, while the sharp dicrotic notch is gradually lost. This increase of systolic pressure with distance from the heart in a tapered tube is a dynamic phenomenon in an elastic branching system. In a steady flow in a rigid tube of similar taper, the pressure must go down in the direction of flow unless there is deceleration. In the present case, however, the *mean* value of the pressure, averaged over the period of a heartbeat, still decreases with increasing distance from the aortic valve. It is difficult to see it in Figure 3.13:2 because the fall in mean pressure is only about 4 mm Hg (0.5 kPa) in the

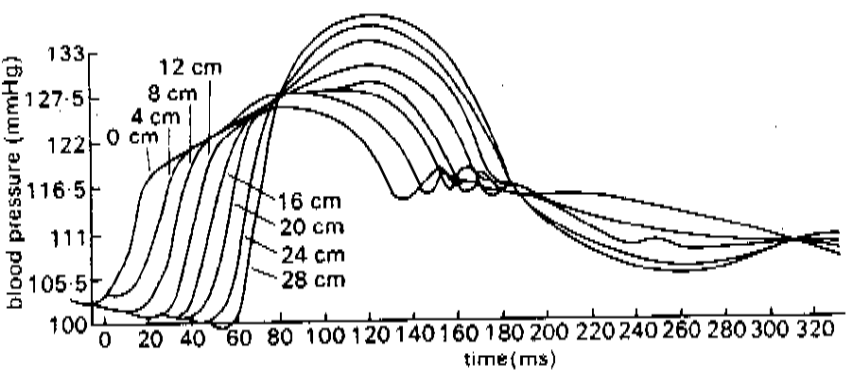

FIGURE 3.13:2. Simultaneous blood pressure records made at a series of sites along the aorta in the dog, with distance measured from the beginning of the descending aorta. From Olson, R.M. (1968) Aortic blood pressure and velocity as a function of time and position. *J. Appl. Physiol.* **24**: 563–569. Reproduced by permission.

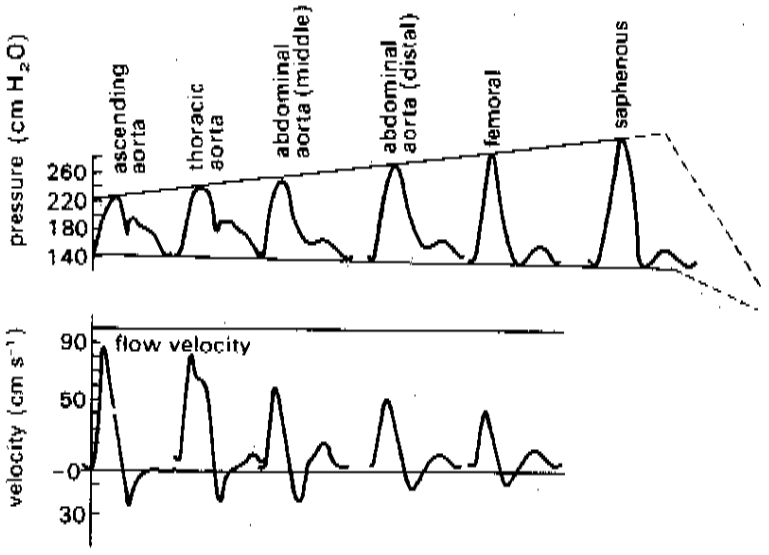

FIGURE 3.13:3. Pressure and velocity waves at different sites in the arteries of a dog. From McDonald (1974), by permission.

whole length of the aorta, while the amplitude of the pressure oscillation between systole and diastole nearly doubles.

This process of amplification of the pressure pulse continues into the branches of the aorta, as illustrated in Figure 3.13:3. In the dog, it continues to about the third generation of arterial branches. Thereafter both the oscillation and the mean pressure decrease gradually downstream along the arterial tree until it reaches the level of microcirculation.

Figure 3.13:3 also shows the variation of the flow velocity along the aorta. That the pressure and velocity waves are different is an indication of reflection of waves at junctions. The velocity waves do not steepen with distance, nor does the peak systolic velocity increase downstream.

3.14 Effect of Taper

One of the simplifying assumptions made in the preceeding sections is that the tube is circular and cylindrical in shape and is straight. Real blood vessels are often curved and of variable cross section. The nonuniform cross-sectional area is associated with branching (see Sec. 3.1) and elastic deformation of the vessel wall in response to a nonuniform pressure with a finite gradient (see Sec. 3.4). The taper is generally very mild, and it is possible to evaluate its effect approximately without extensive calculations.

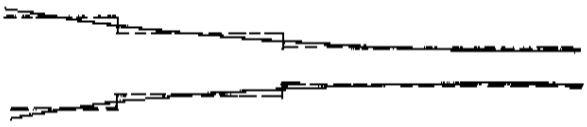

FIGURE 3.14:1. Approximation of a stepwise tapered tube by a continuously tapered blood vessel.

Let a smoothly tapered tube be approximated by a stepwise tapered tube, as shown in Figure 3.14:1. Each site of step change may be regarded as a junction of two tubes, and the method of analysis presented in Section 3.11 can be applied. We have learned in Section 3.11 that the rate of energy transfer in a reflected wave is proportional to the square of $\mathcal{R}$, and therefore if $\mathcal{R} \ll 1$ it is quite negligible. $\mathcal{R}$, in this case, as is given in Eq. (3.11:8), is proportional to the difference in cross-sectional areas of the two segments divided by the sum of the cross-sectional areas, and is obviously very small if the taper is mild. $\mathcal{R}^2$ is another order of magnitude smaller. Therefore we conclude that very little energy is reflected as the wave travels along a slowly varying tube, and we may analyze the wave's development as if all the energy were transmitted.

The rate of transfer of energy in a progressive wave across any cross section of a vessel is shown in Eq. (3.11:10) to be equal to p^2/Z, the square of the oscillatory pressure divided by the characteristic impedance of the tube. If all the energy is transmitted, then p^2/Z is a constant and we have

$$p = \text{const.} \cdot Z^{1/2}. \tag{1}$$

Thus, in a gradually tapering artery, the amplitude of the pressure wave is proportional to the square root of the characteristic impedance. Since the characteristic impedance is $\rho c/A$, we see that Z increases as A decreases if ρc were constant. Hence the amplitude of the pressure wave increases as the wave propagates down a tapering tube with decreasing cross section. The amplitude of the aortic *flow* pulse, proportional to p/Z [see Eq. (3.11:5)], will correspondingly decrease, being proportional to $Z^{-1/2}$.

These predicted features are evident in the records shown in Figures 3.13:2 and 3.13:3. However, a quantitative comparison of the predictions with the experimental results shows that the peaking is overestimated by the theory. One of the reasons for this is the neglecting of viscous effects of the blood and blood vessel; the other reason is the inaccuracy of the theory. The theory is more accurate if the taper is small. But how small is small? To answer this question one should turn to mathematics. We can reduce the general equations of motion and boundary conditions to a dimensionless form. Then we recognize two characteristic lengths, the tube radius and the wave length. For the taper, the proper dimensionless parameter is the rate of change of tube radius per unit wavelength. If this rate is not very small, the theory is not very accurate. Let $\xi = x/\lambda$, where x is the

axial coordinate and λ is the wavelength, and let $D_r = D/D_0$, the ratio of the blood vessel at x to that at the entry section $x = 0$. Then the preceding description means that the effect of taper is to be judged by the derivative $dD_r/d\xi$. Now

$$\frac{dD_r}{d\xi} = \frac{dD_r}{dx}\frac{dx}{d\xi} = \lambda\frac{dD_r}{dx} = \frac{\lambda}{D_0}\frac{dD}{dx}. \tag{2}$$

Hence the effective taper is the product of the wavelength λ, expressed in tube diameter at the entry, and the rate of change of the diameter dD/dx.

Now, in the case of the aorta, the wavelength of the first few harmonics is longer than the length of the aorta, and the effective taper $dD_r/d\xi$ may be fairly large by virtue of large values of λ/D_0. For these harmonics the inaccuracy of the simple theory may have led to the overestimation of the peaking mentioned earlier.

Problem

3.27 The cross-sectional area of the abdominal aorta is about 40% of the area of the thoracic aorta. The Young's modulus is about twice that of the thoracic aorta. Show that the ratio of the characteristic impedances in these aorta is 3.5 and that the pressure pulse amplitude in the abdominal aorta is expected to be 85% higher than that in the thoracic aorta. How much additional increase in pressure pulse amplitude is expected because of the reflection of the wave at the iliac junction?

3.15 Effects of Viscosity of the Fluid and Viscoelasticity of the Wall

At the beginning of this chapter we analyzed steady flow of a viscous fluid in tube. In Sections 3.8 to 3.12, however, we treated pulsatile flow of blood as if it has no viscosity. The major justification for this has been suggested in Section 3.9 namely, that in human arterial blood flow the Reynolds and Womersley numbers are much larger than 1 in the large arteries, so that the boundary layers are very thin campared with the vessel radius. The boundary layers mediate the ideal fluid solution to the real fluid no-slip condition on the solid wall. The Reynolds and Womersley numbers decrease toward the periphery, become smaller than 1 in arterioles, capillaries, and venules. Hence the influence of viscosity is felt more and more as blood flows toward the peripheral vessels. In the microcirculation the entire flow field is dominated by viscous stresses.

Even in large arteries, where the Reynolds and Womersley numbers are large, the viscosity of the fluid still has a profound influence. Viscous stresses play a dominant role in determining stability and turbulence in the

arteries, and in determining whether the streamline will separate (diverge) from the wall of the vessel at branching points or at segments where a sudden change in cross section occurs, such as in stenosis or aneurysm.

Physically, because viscosity is a dissipation mechanism, one expects that it would reveal itself in the attenuation of velocity and pressure in the direction of propagation. Associated with attenuation will be phase changes. As far as their effect on the wave propagation is concerned, the effect of viscoelastic dissipation in the vessel wall is found to be more significant than the viscous dissipation of the blood.

To include viscosity of blood and viscoelasticity of the vessel wall in the pulsatile flow analysis, consider large arteries and make the following simplifying hypotheses:

a. The fluid is homogeneous and Newtonian.
b. The wall material is isotropic and linearly viscoelastic.
c. The fluid motion is laminar.
d. The motion is so small that squares and higher order products of displacements and velocities, and their derivatives, are negligible.

Then the field equations are the linearized Navier–Stokes equations for the blood, the linearized Navier's equation for the wall, and the equation of continuity. The boundary conditions are the continuity of shear and normal stresses and velocities at the fluid–solid interface, and appropriate conditions on the external surface of the tube and at the ends of the tube. The governing equations are given in Section 2.6 in rectangular cartesian coordinates. Changing to polar coordinates to describe an axisymmetric traveling wave in a tube of incompressible viscoelastic material, we have, for the fluid,

$$\frac{\partial v_r}{\partial t} = -\frac{1}{\rho}\frac{\partial p}{\partial r} + \nu\left(\frac{\partial^2 v_r}{\partial r^2} + \frac{1}{r}\frac{\partial v_r}{\partial r} - \frac{v_r}{r^2} + \frac{\partial^2 v_r}{\partial x^2}\right), \tag{1}$$

$$\frac{\partial v_x}{\partial t} = -\frac{1}{\rho}\frac{\partial p}{\partial x} + \nu\left(\frac{\partial^2 v_x}{\partial r^2} + \frac{1}{r}\frac{\partial v_x}{\partial r} + \frac{\partial^2 v_x}{\partial x^2}\right), \tag{2}$$

$$\frac{\partial v_x}{\partial x} + \frac{\partial v_r}{\partial r} + \frac{v_r}{r} = 0, \tag{3}$$

and, for the tube wall,

$$\frac{\rho_w}{\mu^*}\frac{\partial^2 u_r}{\partial t^2} = \frac{\partial^2 u_r}{\partial r^2} + \frac{1}{r}\frac{\partial u_r}{\partial r} - \frac{u_r}{r^2} + \frac{\partial^2 u_r}{\partial x^2} - \frac{1}{\mu^*}\frac{\partial \Omega}{\partial r}, \tag{4}$$

$$\frac{\rho_w}{\mu^*}\frac{\partial^2 u_x}{\partial t^2} = \frac{\partial^2 u_x}{\partial r^2} + \frac{1}{r}\frac{\partial u_x}{\partial r} + \frac{\partial^2 u_x}{\partial x^2} - \frac{1}{\mu^*}\frac{\partial \Omega}{\partial x}, \tag{5}$$

$$\frac{\partial u_x}{\partial x} + \frac{\partial u_r}{\partial r} + \frac{u_r}{r} = 0, \tag{6}$$

where v_x, v_r, v_θ are the velocity components of the fluid; u_x, u_r, u_θ are the displacement components of the wall; μ^* is the dynamic modulus of rigidity of the wall; and Ω is a pressure, which must be introduced since we have assumed the material to be incompressible. ν is the *kinematic viscosity* of the blood, μ is the coefficient of viscosity, ρ is the density of the blood, ρ_w is the density of the wall material, and $\nu = \mu/\rho$.

If the external surface of the tube is stressfree, and if the inner and outer radii of the tube are a and b, respectively, then the boundary conditions are

$$v_r = 0 \qquad \text{at } r = 0, \tag{7}$$

$$\partial v_x/\partial r = 0 \qquad \text{at } r = 0, \tag{8}$$

$$v_r = \partial u_r/\partial t \qquad \text{at } r = a, \tag{9}$$

$$v_x = \partial u_x/\partial t \qquad \text{at } r = a, \tag{10}$$

$$\mu\left(\partial v_r/\partial x + \partial v_x/\partial r\right) = \mu^*\left(\partial u_r/\partial x + \partial u_x/\partial r\right) \qquad \text{at } r = a, \tag{11}$$

$$-p + 2\mu\left(\partial v_r/\partial r\right) = -\Omega + 2\mu^*\left(\partial u_r/\partial r\right) \qquad \text{at } r = a, \tag{12}$$

$$\mu^*\left(\partial u_r/\partial x + \partial u_x/\partial r\right) = 0 \qquad \text{at } r = b, \tag{13a}$$

$$-\Omega + 2\mu^*\left(\partial u_r/\partial r\right) = 0 \qquad \text{at } r = b. \tag{13b}$$

The solution that satisfies the boundary conditions (7) and (8) may be posed in the following form*:

$$v_x = -\sum_{n=0}^{N} i\left\{A_1\gamma_n J_0\left(i\gamma_n r\right) + A_2\kappa_n J_0\left(i\kappa_n r\right)\right\}\exp i\left(n\omega t - \gamma_n x\right), \tag{14}$$

$$v_r = -\sum_{n=0}^{N} i\gamma_n\left\{A_1 J_1\left(i\gamma_n r\right) + A_2 J_1\left(i\kappa_n r\right)\right\}\exp i\left(n\omega t - \gamma_n x\right), \tag{15}$$

$$p = \sum_{n=0}^{N} A_3 J_0\left(i\gamma_n r\right)\exp i\left(n\omega t - \gamma_n x\right), \tag{16}$$

$$u_r = \sum_{n=0}^{N} -i\gamma_n\left\{A_4 J_1\left(k_n r\right) + B_4 Y_1\left(k_n r\right) + A_5 J_1\left(i\gamma_n r\right) + B_5 Y_1\left(i\gamma_n r\right)\right\}\cdot\exp i\left(n\omega t - \gamma_n x\right), \tag{17}$$

$$u_x = \sum_{n=0}^{N} -\left\{k_n A_4 J_0\left(k_n r\right) + k_n B_4 Y_0\left(k_n r\right) + i\gamma_n A_5 J_0\left(i\gamma_n r\right) + i\gamma_n B_5 Y_0\left(i\gamma_n r\right)\right\}\cdot\exp i\left(n\omega t - \gamma_n x\right), \tag{18}$$

$$\Omega = \sum_{n=0}^{N}\left\{A_6 J_0\left(i\gamma_n r\right) + B_6 Y_0\left(i\gamma_n r\right)\right\}\exp i\left(n\omega t - \gamma_n x\right), \tag{19}$$

* In a strict notation the A's and B's should have a subscript n because their values may be different for each n.

where ω is the angular frequency, n is the harmonic number, γ_n is a constant named the *propagation constant* of the nth harmonic, N is a constant, the A's and B's are complex constants, J_0 and J_1 are Bessel functions of the first kind, Y_0 and Y_1 are Bessel functions of the second kind, and

$$\kappa_n^2 = \left(in\omega/\nu\right) + \gamma_n^2, \quad k_n^2 = n^2\omega^2\rho_w/\mu^* - \gamma_n^2. \tag{20}$$

$$A_4 = \left(i/n\omega\rho\right)A_3, \quad A_6 = n^2\omega^2\rho_w A_5, \quad B_6 = n^2\omega^2\rho_w B_5. \tag{21}$$

When these solutions are substituted into the boundary conditions (9) to (13), six linear, homogeneous, and simultaneous equations in six unknown coefficients, $A_1, A_2, \ldots, B_5$, are obtained. For a nontrivial solution the determinant of the coefficients of $A_1, A_2, \ldots, B_5$ must vanish. This determinantal equation,

$$\Delta\left(\gamma_n, \kappa_n, k_n, \mu, \mu^*, a, b\right) = 0, \tag{22}$$

is the frequency equation for the pulse wave. If $\gamma_n = \beta + i\alpha$ is solved with other parameters assigned, then β is the *wave number*, α is the *attenuation coefficient*, and $C_p = \omega/\beta$ is the *phase velocity*.

The dynamic elastic modulus of the vessel wall, μ^*, is a complex number if the wave motion is represented by complex exponential functions listed in Eqs. (14) to (19). Since μ^* is complex, the solution γ_n is almost certain to be complex also, thus yielding the attenuation coefficient in association with each characteristic wave number. It is evident that extensive numerical calculations are necessary to obtain detailed information.

One thing that becomes evident from the general equations is that Eq. (22) has many solutions. One of them is akin to the *flexural mode* discussed in Section 3.8 and is an improvement of that solution. All the others are new modes not considered before in this book. These include *longitudinal modes*, in which the principal motion consists of motion of the vessel wall in the longitudinal direction; *torsional modes*, in which the principal motion is the torsional oscillation of the vessel wall; and higher modes of these three types with higher frequencies, shorter wavelengths, and different attenuation. Many of these theoretical wave types have been found in in vivo measurements.

A general reader would probably have little interest in the numerical details and is thus referred to the original papers. Furthermore, it is possible to relax some or all of the simplifying assumptions listed earlier and to study mathematically the arterial blood flow problem in greater depth. A great deal has been published. Historically, Euler (1775) was the first to write down the governing equations of arterial blood flow. He suggested that the relationship between blood pressure p and cross-sectional area A be represented by $A = A_0 p(c + p)^{-1}$ or $A = A_0(1 - e^{-p/c})$. Euler's equations were solved later by Lambert (1958). Young (1808, 1809) was the first to derive the wave speed formula given in Section 3.8, Eq. (15). Lamb (1897–1898) derived phase velocities of two types of long waves in arterial

wall. Joukowsky (1900) used Riemann's method of characteristics to solve Euler's equation. Witzig (1914) was the first to investigate the effect of fluid viscosity. Hamilton and Dow (1939) studied the relationship between arterial pulse waves and cardiac ejection and stroke volume of the heart. Jacobs (1953) was the first to investigate the effect of arterial wall mass and nonlinear elasticity as well as fluid viscosity. King (1947), Morgan and Kiely (1954) and Morgan and Ferrante (1955) were the first ones to investigate the effect of viscoelasticity. Womersley (1955a,b) compared theory with experiments, considered tethering, branching, and longitudinal variation of the cross-sectional area, and gave exhaustive attention to computational details. Landowne (1958) experimentally induced waves in human brachial and radial arteries. Taylor (1959, 1966a,b) used impedance methods and electric analogs. McDonald (1960) made thorough examinations of theories and experiments from a physiological point of view. Klip (1958, 1962, 1967) presented extensive studies on measuring techniques, effects of fluid viscosity, wall thickness, elasticity, viscoelasticity, and three modes of axisymmetric and asymmetric waves. Rubinow and Keller (1972) paid attention to the effect of external tissues, and found significant effects. Anliker and Raman (1966), Anliker and Maxwell (1966), Jones et al (1971), and Maxwell and Anliker (1968) studied Korotkof sound, dispersion, initial strain, and found axisymmetric waves mildly dispersive, asymmetric waves highly dispersive. Van der Werff (1973) developed a periodic method of characteristics. Pedley (1980) has given a thorough review of recent advances in the theory of blood flow in large arteries. Extensive review and bibliography are given in Attinger (1964), Bergel (1972), Patel and Vaishnav (1980), Sramek et al. (1995), Valenta (1993), and Wetterer and Kenner (1968).

3.16 Influence of Nonlinearities

Of all the effects, the most difficult one to evaluate is the effect of nonlinearities. In Euler's equation of motion [Eq. (13) of Section 2.6], the connective acceleration term, Dv_i/Dt, is nonlinear, and it is the principal difficulty of hydrodynamics. The viscous force term, $\partial\sigma_{ij}/\partial x_j$, becomes nonlinear if the constitutive equation of the fluid is non-Newtonian. Blood is non-Newtonian, and the effect of nonlinear blood viscosity is especially important with regard to flow separation at points of bifurcation in pulsatile flow. In the equation governing the blood vessel wall, the most significant nonlinearity comes from the finite strain and nonlinear viscoelasticity.

To check the effects of nonlinearity means to compare the solutions of the linearized equations and boundary conditions with those of nonlinear ones. This is usually impossible because the available solutions of nonlinear problems are limited. Sometimes, however, we can discuss the effects of nonlinearity on the basis of dimensional analysis and comparison with experimental evidence. Several examples follow.

Convective Acceleration in Wave Propagation

In the wave analysis of Section 3.8, the local convective acceleration $u_j(\partial u_i/\partial x_j)$ is neglected against the transient acceleration $\partial u_i/\partial t$. Now, let $\tilde{u}$ represent a characteristic velocity of the disturbed flow due to wave motion, ω the circular frequency of the wave, and c the wave speed relative to the mean flow. Then the period of oscillation is $2\pi/\omega$, the wavelength is $2\pi c/\omega$, and the orders of magnitude of the two accelerations are

$$\text{Transient,} \quad \frac{\partial u_i}{\partial t}: \quad \frac{\tilde{u}}{(2\pi/\omega)}, \tag{1}$$

$$\text{Convective,} \quad u_j\frac{\partial u_i}{\partial x_j}: \quad \bar{u}\frac{\tilde{u}}{(2\pi c/\omega)}. \tag{2}$$

Hence the condition that the convective acceleration is negligible compared with the transient acceleration is that (2) $\ll$ (1), that is, if

$$\frac{\tilde{u}}{c} \ll 1. \tag{3}$$

In large arteries, the maximum value of $\tilde{u}/c$ is about 0.25, which is large enough to suggest nonlinear effects. In smaller peripheral arteries, the linearity condition is better justified. In certain rare disorders the arterial wall becomes floppy and c is so low that $\tilde{u}/c$ approaches 1. In aortic valve incompetence, the upstroke of the pulse wave becomes very steep, $\tilde{u}$ becomes quite large, and a nonlinear effect is expected. The effect is to increase acceleration and pressure drop. The pressure wave form is therefore steepened at the peak of the velocity wave and flattened at the valley.

Effect of Nonlinear Elasticity of Vessel Wall on Wave Propagation

The incremental Young's modulus of the arterial wall increases with the tensile stress in the vessel wall. An increase in Young's modulus of the vessel wall increases the wave speed [see Eq. (3.8:15)]. Experimental evidence for this is shown in Figure 3.16:1, which was obtained by Anliker (1972) using short trains of high-frequency pressure oscillations generated in the dog aorta and superposed on pulse waves. The wavelength of such high-frequency oscillations is short, so that several cycles can be recorded at a downstream observation site before the reflected wave from the iliac junction returns to that site and distorts the recording. The results show that the wave speed is higher in systole than in diastole. This is due partly to the increase in the speed of the progressive waves, c, and partly to the higher mean flow velocity, $U(t)$, at systole. According to Section 3.10, pressure perturbations superposed on a steady flow have a velocity of propagation equal to the velocity c plus the steady flow velocity.

Apply the same principle to a single harmonic pressure wave. At a peak (high pressure) the velocity of propagation is higher than the mean veloc-

3.20 Messages Carried in the Arterial Pulse Waves and Clinical Applications

Clinical applications of pulse wave studies are generally aimed at the following:

a. Discovering and explaining diseases of the arteries such as atherosclerosis, stenosis, and aneurysm. Locating sites that need surgical treatment.
b. Inferring the condition of the heart.
c. Diagnosing diseases anywhere in the body.

The approach to any of these objectives is to extract information from the characteristics of the waves. The most ancient method is to use fingers as probes. Any abnormality in the condition of the body affects pulse waves, which carry the message from distant sites.

The idea of extracting information from the arterial pulse waves to gain information about the heart and other organs of the body, however, remains an ideal. If we were able to read all the messages in the arterial pulse waves, then all we need for noninvasive diagnosis is to observe these waves in some conveniently located arteries (such as the radial artery on the wrist). If the messages are clear and unequivocal, then the art of noninvasive diagnosis would have been moved ahead a big step.

The idea of using pulse waves for diagnosis has been with us for a long time. In China, the oldest classic on arterial pulse waves is the *Nei Jing* (內經) mentioned in Chapter 1, Section 1.10. It was followed by *Nan Jing* (難經, first or second century B.C., authorship attributed to Qin Yue-Ren, 秦越人). *Jing* means classic, *Nan* means difficult as an adjective, or question as a verb). The book of Nan Jing sought to answer difficult questions, including those concerned with pulse waves. In the Eastern Han Dynasty, Chang Chi (張機, 字仲景) (probably 150 to 219 AD) wrote the books *The Influence of External Factors* (傷寒論) and the *Abstracts of the Golden Chest* (金匱要略), which systematically organized the Han Dynasty's 300 years' clinical experience in using pulse waves in diagnosis. Then in Tzin Dynasty (晉代), Wang Shu-He (王叔和) (201 to 285 AD) wrote *Mai Jing*, the *Book on Pulse Waves* (脈經). These became the classics of Chinese medicine, and their ideas and methods have been continuously developed and are being used in the Orient to this day.

The presentations given in these classics are descriptive and speculative, using similes and words to describe and classify the pulse waves. Empirically, abnormal waves were related to disease states. Clearly, the tasks of good recording, clear analysis, physiological experimentation, and rational explanation are left to modern researchers! The author's beginning studies are very limited in scope [Dai et al. (1985), Xue and Fung (1989)]. A large literature exists in Chinese.